AD NUMBER

AD803548

LIMITATION CHANGES

TO:

Approved for public release; distribution is unlimited.

FROM:

**Distribution authorized to U.S. Gov't. agencies and their contractors;
Administrative/Operational Use; 14 NOV 1966.
Other requests shall be referred to Office of Naval Research, Physics Branch, Department of the Navy, Washington 25, DC.**

AUTHORITY

ONR notice, 27 Jul 1971

IITRI Project No. A6145

(Annual Summary Report No. 1)

on

EXCESS NOISE IN SEMICONDUCTORS

Contract No. NOOO14-66-C0032

James J. Brophy

IIT Research Institute
10 West 35th Street
Chicago, Illinois 60616

IITRI Project No. A6145

(Annual Summary Report No. 1)

on

EXCESS NOISE IN SEMICONDUCTORS

Contract No. NOOO14-66-C0032

James J. Brophy

for

Office of Naval Research
Department of the Navy
Washington 25, D. C.

Attention: Mr. F. B. Isakson, Head,
Physics Branch

Covering the period of November 15, 1965 to November 14, 1966

November 14, 1966

IIT RESEARCH INSTITUTE

TABLE OF CONTENTS

EXCESS NOISE IN SEMICONDUCTORS

ABSTRACT

Optical emission fluctuations from a GaAs and a Ga(AsP) luminescent diode, as well as from a GaAs junction laser, have been measured. Correlation is observed between optical emission noise and forward current noise of the diode, suggesting that carrier transitions responsible for both effects are the same. Diodes in which considerable carrier recombination occurs in the space charge region exhibit characteristic time constants in both the optical noise and forward current noise. More heavily doped junctions in which tunneling dominates yield only 1/f noise spectra. Only photon noise is observed from diodes in which the junction current is by carrier diffusion.

It is possible to measure non-destructively all important p-n junction parameters of luminescent diodes by judicious choice of experimental techniques. Thus, the junction area, width, internal potential, saturation current, and impurity content can be determined. This facility results from the application of standard electrical measurements coupled with optical properties of such diodes.

Additional work carried out on optical absorption fluctuations in germanium shows that previous unsuccessful experimental attempts to detect the effect are consistent with the analytical prediction of the magnitude. Finally, preliminary experimental noise measurements in single-crystal CdTe suggest that the dominant effect is shot noise associated with internal inhomogeneities.

EXCESS NOISE IN SEMICONDUCTORS

I. INTRODUCTION

Random fluctuation effects in solid materials can be used effectively as a tool to understand physical mechanisms underlying the behavior of solids. Noise phenomena are also important in semiconductor devices since the inherent noise level determines the limit of sensitivity in practical applications. This research program emphasizes the application of noise techniques to better understanding of semiconductors but results of direct interest in connection with devices are also obtained.

This Annual Summary Report No. 1 describes the work performed under Contract No. NOOO14-66-C0032, during the period of November 15, 1965 to November 14, 1966. During this period, we have completed a study of optical emission fluctuations from luminescent p-n junctions, including laser diodes operated below the lasing threshold. In addition, continued effort on optical emission fluctuations in germanium was maintained and preliminary information concerning electrical noise effects in single crystal cadmium telluride was developed.

II. TECHNICAL DISCUSSION

A. Optical Emission Fluctuations

It is well established that characteristic features of the electrical noise spectrum in semiconductors and semiconductor p-n

junctions can be used to derive important information about electronic transition probabilities. In the case of luminescent p-n junctions and injection lasers, such fluctuations are expected in the optical emission if the carrier transitions responsible for current noise are accompanied by photon emission. This expectation has been confirmed by the study of optical emission fluctuations and current noise in electroluminescent p-n junctions.

As reported in detail in Appendix I, such optical emission fluctuations are observed and they are correlated with the forward current noise of the diode. In favorable cases the electronic transition probabilities for photon emission can thus be determined. The noise spectra of all the units examined, however, do not exhibit such effects. For example, 1/f optical noise associated with 1/f junction noise is observed in some units while in other cases no noise beyond statistical photon noise can be detected.

It is possible to relate the different noise characteristics of luminescent diodes with the dominant mechanism of current flow across the junction. Useful characteristic features are found in the noise spectra when carrier recombination transitions occur in the junction space charge region. Other current transport mechanisms such as tunneling and diffusion do not lead to such useful noise spectra.

This work establishes the presence of optical emission fluctuations from electroluminescent diodes and shows how such measurements may be interpreted in terms of carrier transitions and current transport at the junction.

B. Characteristics of p-n Junctions

During the course of the above work, it became necessary to establish parameters of the p-n junctions in order to relate them to observed noise effects. It was important to determine these parameters non-destructively so that the diodes would be available for subsequent measurements. Fortunately, because of the optical properties of such units, it proves possible to determine essentially all of the important p-n junction parameters through a combination of electrical and optical measurements.

This work is described in Appendix II and shows that the junction area, width, internal potential, saturation current, and impurity content may all be determined. In addition, the junction parameters important for the many useful applications of semiconductor p-n junctions (rectifiers, voltage regulators, capacitors, photocells, nuclear radiation detectors, photoelectric generators, light sources, lasers, etc.) are clearly illustrated by the measurements.

A major reason for the success of these measurements is the good quantitative agreement between experimental observations and simple p-n junction semiconductor theory. Therefore, the studies are described separately since they may be useful pedagogically to other workers interested in p-n junctions and to beginners in semiconductor physics and solid state electronics.

C. Other Noise Studies

The noise properties of photomultiplier tubes were determined as part of the study of luminescent p-n junctions. This was necessary in order to separate photomultiplier noise from the desired optical emission noise. Although the noise properties of photomultiplier tubes are quite well established, the present specific results are recorded in Appendix III for possible future reference. In addition, we point out that because of the well established noise effects in photomultipliers, noise measurements provide a convenient way for determining the secondary multiplication gain. It does not appear that this observation has been noted previously.

For some time we have undertaken several measurements to detect optical absorption fluctuations in single crystal germanium. Such fluctuations are expected because of free carrier absorption and the carrier fluctuations associated with 1/f current noise. Appendix IV is a simple though more careful analysis of the phenomenon than previously reported. It confirms that previous experimental techniques were not sensitive enough to be successful. Based on this work, a new experimental design of sufficient sensitivity has been completed. A description of this experimental approach is contained in the proposal submitted for continuation of the program. Although careful attention to experimental details is necessary, we believe the experiment is feasible and of sufficient interest to pursue.

A fairly large number of different semiconducting materials have been investigated for their noise properties in the past. Such a study has never been made of cadmium telluride, however, in spite of the interesting characteristics of this crystal and the fact that it has important potential applications. A preliminary study of current noise in single crystal CdTe is reported in Appendix V. It is found (not surprisingly) that contact noise effects are extremely important. It is possible, however, to measure bulk noise effects independent of the contacts. The noise results in hand to date suggests that the observed noise is simple shot noise, at least in the high resistivity specimens. If this is confirmed by further work, the noise properties of cadmium telluride are significantly different from those in analogous crystals such as cadmium sulfide.

III. RECOMMENDATIONS FOR FUTURE WORK

As discussed in the proposal for the continuation of the present program, it is recommended that optical absorption fluctuations in single crystal germanium be continued. Based on our confidence in the validity of the present analytical predictions, we believe that a careful experimental design will succeed in measuring such fluctuations. This work is of interest in connection with the interaction of optical energy in solids and also provides a new experimental tool to study 1/f noise.

In addition, the intriguing preliminary results obtained on current noise in single crystal CdTe indicate that the present work

should be extended. This is so because of the apparently new noise effects in this semiconductor compared to similar crystals and because of the interest in CdTe for device applications.

IV. CONTRIBUTING PERSONNEL AND LOGBOOKS

Samuel L. Webb, Harold N. Spector, William D. Brennan and James J. Brophy have been associated with the program during the past year. Original data for the work performed during the past year can be found in logbook No. C 15167.

V. PUBLICATIONS

The principal investigator presented a paper entitled "Optical Emission Fluctuations from Luminescent PN Junctions" at the June Meeting of the American Physical Society and at the Eighth Fluctuations in Solids Symposium held at the University of Minnesota. Appendix I has been submitted to the Journal of Applied Physics and Appendix II has been submitted to the American Journal of Physics for publication.

VI. SUMMARY

We believe that the research results on optical emission fluctuations from luminescent p-n junctions make a useful contribution to the understanding of such devices, including injection lasers, and to fluctuation phenomena in general. The preliminary results of

electrical noise in CdTe are also intriguing. We continue to be interested in random noise effects in solids and are looking forward to a continuation of the program.

Respectfully submitted,

IIT Research Institute

James J. Brophy
Vice President

APPENDIX I

FLUCTUATIONS IN LUMINESCENT JUNCTIONS

by

James J. Brophy

IIT RESEARCH INSTITUTE

FLUCTUATIONS IN LUMINESCENT JUNCTIONS

by

James J. Brophy
IIT Research Institute
Chicago, Illinois 60616

ABSTRACT

Optical emission fluctuations from three types of GaAs and Ga(AsP) p-n junction luminescent diodes have been examined. Characteristic time constants of 12×10^{-3} and 0.45×10^{-3} seconds are observed in both the optical noise spectra and forward current noise spectra of a GaAs diode in which carrier recombinations occur in the junction space charge region. More heavily doped junctions ($\sim 10^{19}$ cm^{-3}), in which tunnel currents predominate exhibit 1/f noise. In either case, correlation exists between optical emission noise and forward current noise, suggesting that carrier transitions responsible for both effects are the same. Only simple photon noise is observed from a Ga(AsP) diode in which junction diffusion currents are significant, although the forward noise spectrum is also 1/f noise.

I. INTRODUCTION

Carrier transitions responsible for optical radiation from a forward-biased luminescent p-n junction are expected to result in current noise of the junction current and corresponding fluctuations in the optical emission. It is known that the current noise spectra of forward-biased[1] and reverse-biased[2] p-n junctions show characteristic structural features similar to those observed in homogeneous samples. Current noise measurements have been used with considerable quantitative success to study carrier transitions in semiconductor crystals[3] and in p-n junctions.[4] Similar characteristic features are reported here for both the current noise spectrum and optical emission noise spectrum of certain luminescent junctions.

Optical emission fluctuations in electroluminescence have previously been reported for MgO cold cathodes.[5] Correlation between cathode current noise and optical emission noise is observed and attributed to fluctuations in electron tunneling. Also, optical noise of injection lasers has been examined above the lasing threshold.[6] In this case, however, the noise properties are more closely related to laser action than to properties of the p-n junction per se.

II. LUMINESCENT DIODES

Three different types of luminescent diodes have been examined: a GaAs unit, a mixed-crystal GaAs-GaP diode, and a GaAs laser diode (S-41) operated well below threshold. Pertinent characteristics of the junctions are listed in Table 1.* All three are abrupt junctions, as determined from junction capacitance measurements, and carrier concentrations noted refer to the lighter-doped region.

In each case the electroluminescent emission peak occurs at lower energy than the peak of the photoconductive response, Figure 1. This suggests that carrier transitions responsible for photon emission involve localized levels, as generally found for such junctions. The two peaks are closer together in the case of the laser diode compared to the other GaAs unit and the photoresponse curve is much broader. This is consistent with the much greater impurity concentration in this junction.

The slope of the forward current-voltage characteristic is different for each unit, as indicated in the conventional fashion by β in Table 1. The value is nearly equal to 2 in the case of the GaAs unit, indicative of carrier recombination transitions in the junction region;[7] the lower value for the Ga(AsP) diode suggests that significant carrier diffusion across the junction is present; the large β associated

*The Ga(AsP) unit was kindly supplied by Dr. Robert Ruehrwein.

TABLE I

LUMINESCENT DIODE CHARACTERISTICS

Type No.	GAE-420	Ga(AsP)	S-41
Manufacturer	Philco Corp.	Monsanto Co.	Seed Electronics
Material	GaAs	60/40 GaAs/GaP	GaAs
Carrier Concentration cm^{-3}	1×10^{18}	4×10^{17}	$\sim 10^{19}$
Emission Peak eV at 300°K	1.35	1.91	1.36
Photoconductivity Maximum eV at 300°K	1.39	1.97	1.39
Forward β Characteristic	1.9	1.5	5.3
Junction Area cm^2	1.4×10^{-3}	6.5×10^{-4}	1.3×10^{-3}

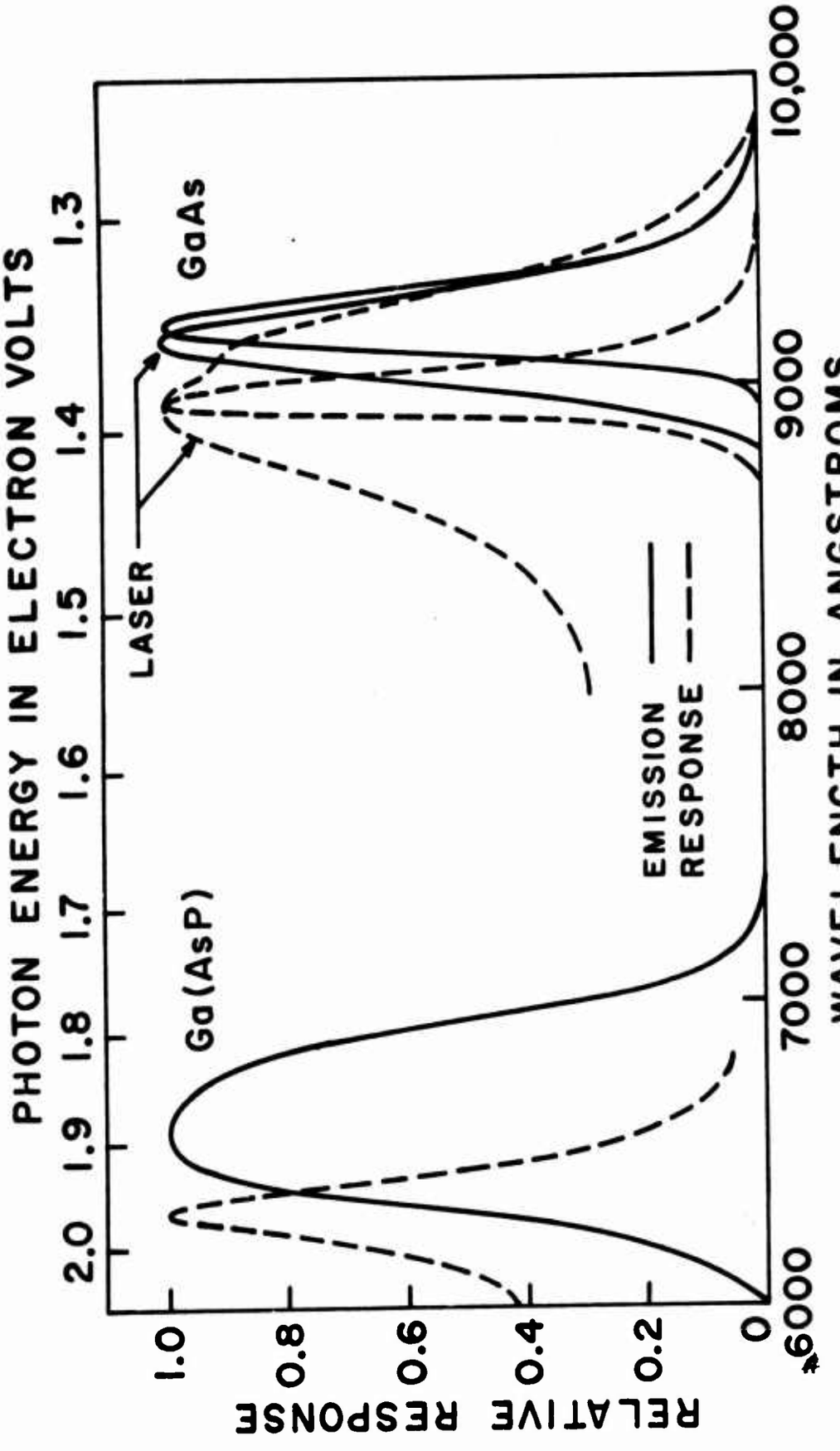

Figure 1. Electroluminescent Emission and Photoelectric Response Spectra of GaAs, Ga(AsP), and GaAs Laser Diodes.

with the diode laser is interpreted to mean that much of the forward current is a result of tunneling transitions. To some extent, these different modes of forward current transport can be correlated with observed junction noise properties.

III. EXPERIMENTAL TECHNIQUE

Diode noise characteristics are examined with the experimental apparatus diagrammed in Figure 2. The diode is energized from a filtered source to eliminate current fluctuations arising in the battery. Current noise in the diode is determined from the voltage appearing across the 10-ohm series resistor. Alternatively, a high turns-ratio input transformer is used in this position to better match the small forward impedance of the junction to the input impedance of the amplifier. This is necessary in cases where the forward current noise is relatively small.

Two silicon photodiodes, Type 1N2175, are positioned to view the optical emission from the GaAs diodes. The silicon photodetectors are replaced by Type 1P21 photomultiplier tubes to examine the Ga(AsP) diode, which emits in the red region of the spectrum. The physical positions of the photodetectors are adjusted so that the photocurrents in each are equal. The output of each detector is fed to identical low-noise amplifier-filter systems of conventional design. The amplified noise output in either channel can be measured with a

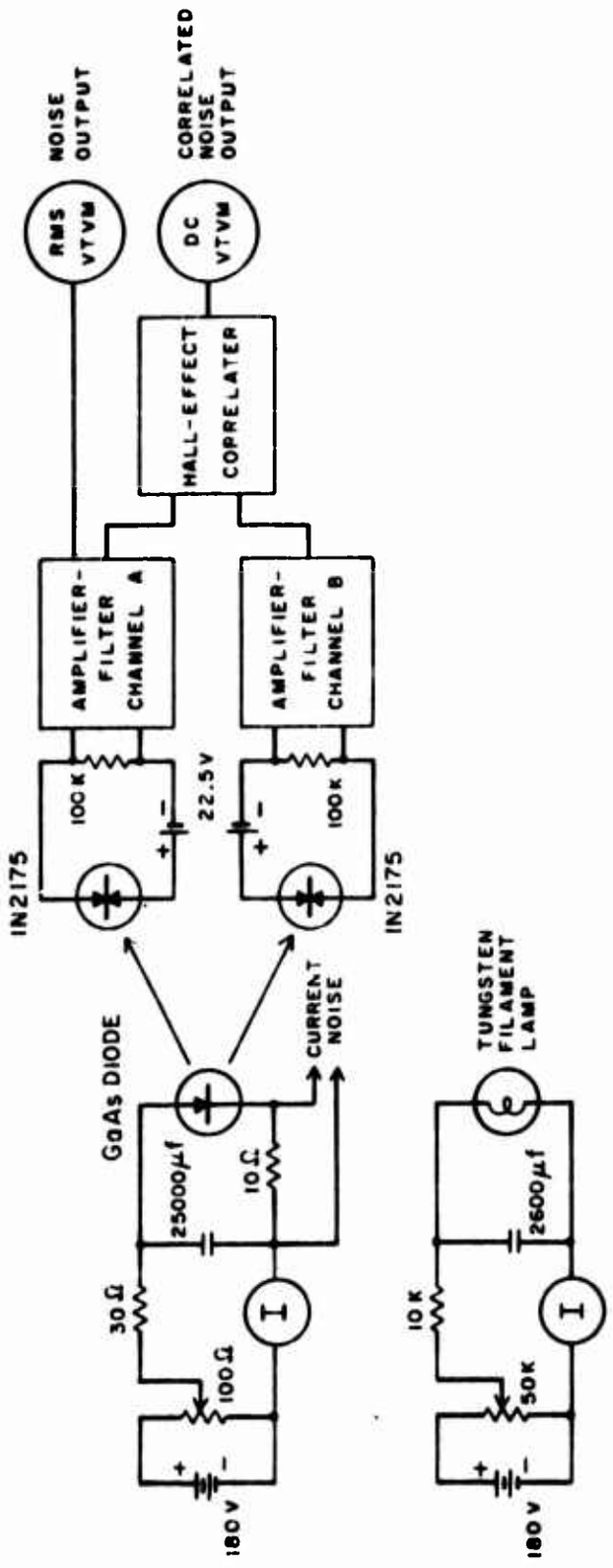

Figure 2. Block Diagram of Experimental Equipment to Measure Optical Emission Fluctuations of a Luminescent Diode.

true rms VTVM for conventional noise measurements. Alternatively, the outputs are cross-correlated in a hall-effect correlator.[8]

Diode current noise measurements and conventional photocurrent noise measurements are made using one amplifier-filter channel. Cross-correlating the outputs of the two photodetectors eliminates effects due to detector noise and reduces the effect of random optical emission of the luminescent diode. It is also possible to obtain the cross-correlation between the photocurrent noise in one detector and the forward current noise of the luminescent junction by connecting the 10-ohm resistor (or input transformer) across one input channel in place of one detector. In this case the wide-band current noise level is attenuated with a potentiometer (not shown) to equal the wide-band photocurrent noise in the other channel.

Each amplifier-filter channel is calibrated using the Nyquist noise of known resistors connected to the amplifier input terminals. Similarly, the cross-correlation mode is calibrated by connecting the two inputs in parallel to known resistors. The correlator is capable of rejecting random noise levels three to four orders of magnitude greater than correlated noise in both channels.[8] Satisfactory operation is also checked by illuminating the photodetectors with tungsten lamp (Figure 1) radiation, which produces purely random optical noise.

IV. EXPERIMENTAL RESULTS

The noise spectra of the GaAs electroluminescent diode GAE-420 are the most interesting of the three examined, both with respect to

optical emission fluctuations and forward current noise. The reverse-bias current noise spectrum, Figure 3, is simple 1/f noise, presumably the result of leakage current at the junction surface. The character of the noise spectrum is not altered by illuminating the diode with white light and the magnitude is considerably in excess of shot noise corresponding to the reverse current.

In contrast, the forward current noise spectrum has structure which suggests at least two discrete characteristic relaxation times. The observed noise level is many orders of magnitude in excess of simple shot noise associated with the forward current, which is $2eI = 5.1 \times 10^{-20}$ amp^2/Hz. Therefore, the shape and magnitude of the forward current noise is attributed to carrier transitions in the region of the junction.

Such structure is not observed in either the Ga(AsP) or the GaAs laser diode, Figure 4 and Figure 5. In these units the forward current noise as well as the reverse-bias current noise spectrum are all 1/f noise. It is not particularly unusual to observe 1/f noise for both the forward and reverse directions in p-n junctions, even when the forward current is a result of tunneling.[9] Comparing the forward spectrum in Figure 3 with those in Figures 4 and 5, it is tempting to associate the observed structure with the fact that carrier recombination in the junction region dominates in the GaAs unit. Presumably, current fluctuations associated with carrier recombinations are masked by ever-present 1/f noise in the other junctions.

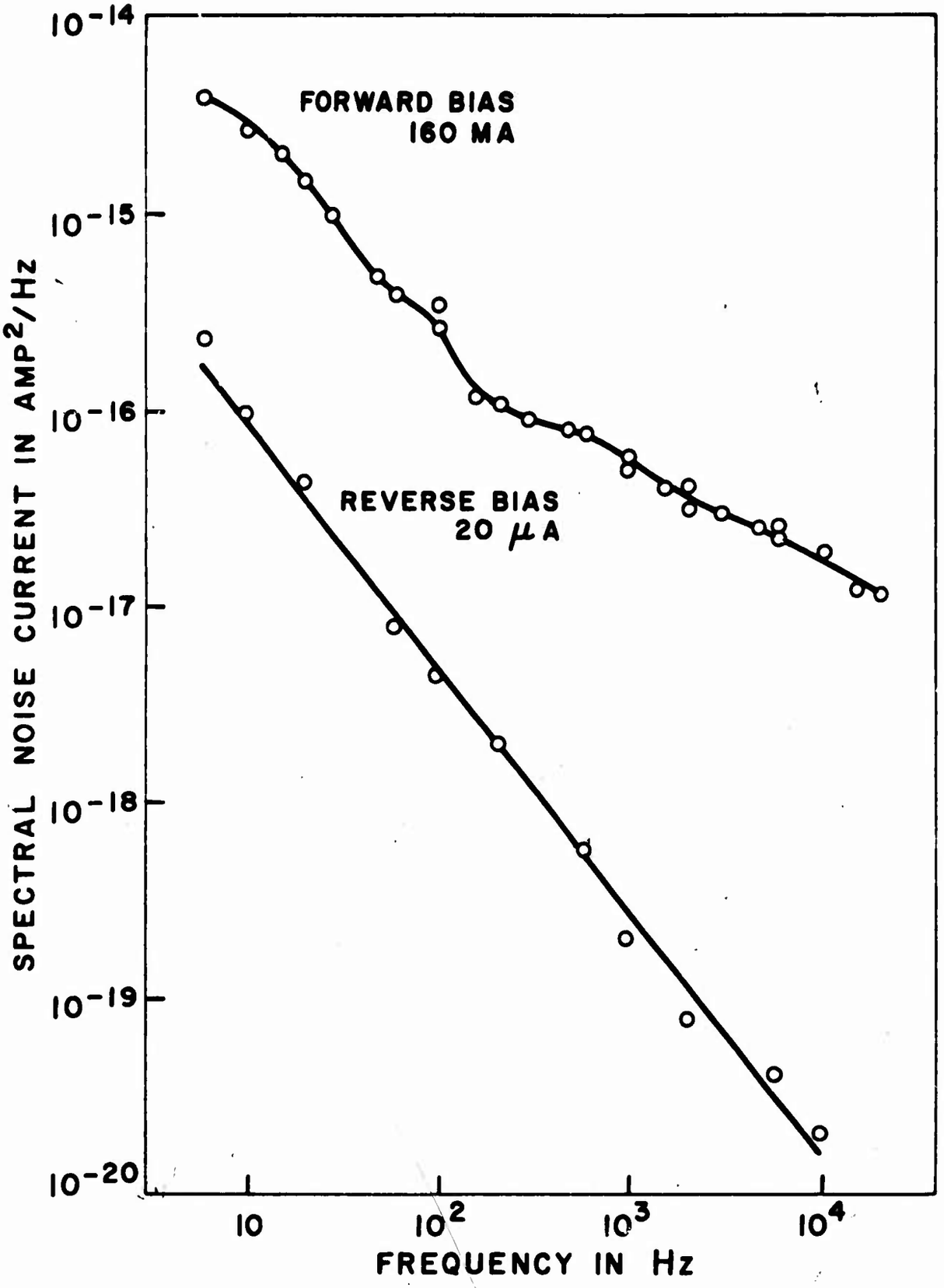

Figure 3. Forward and Reverse Current Noise Spectra of GaAs Luminescent Diode.

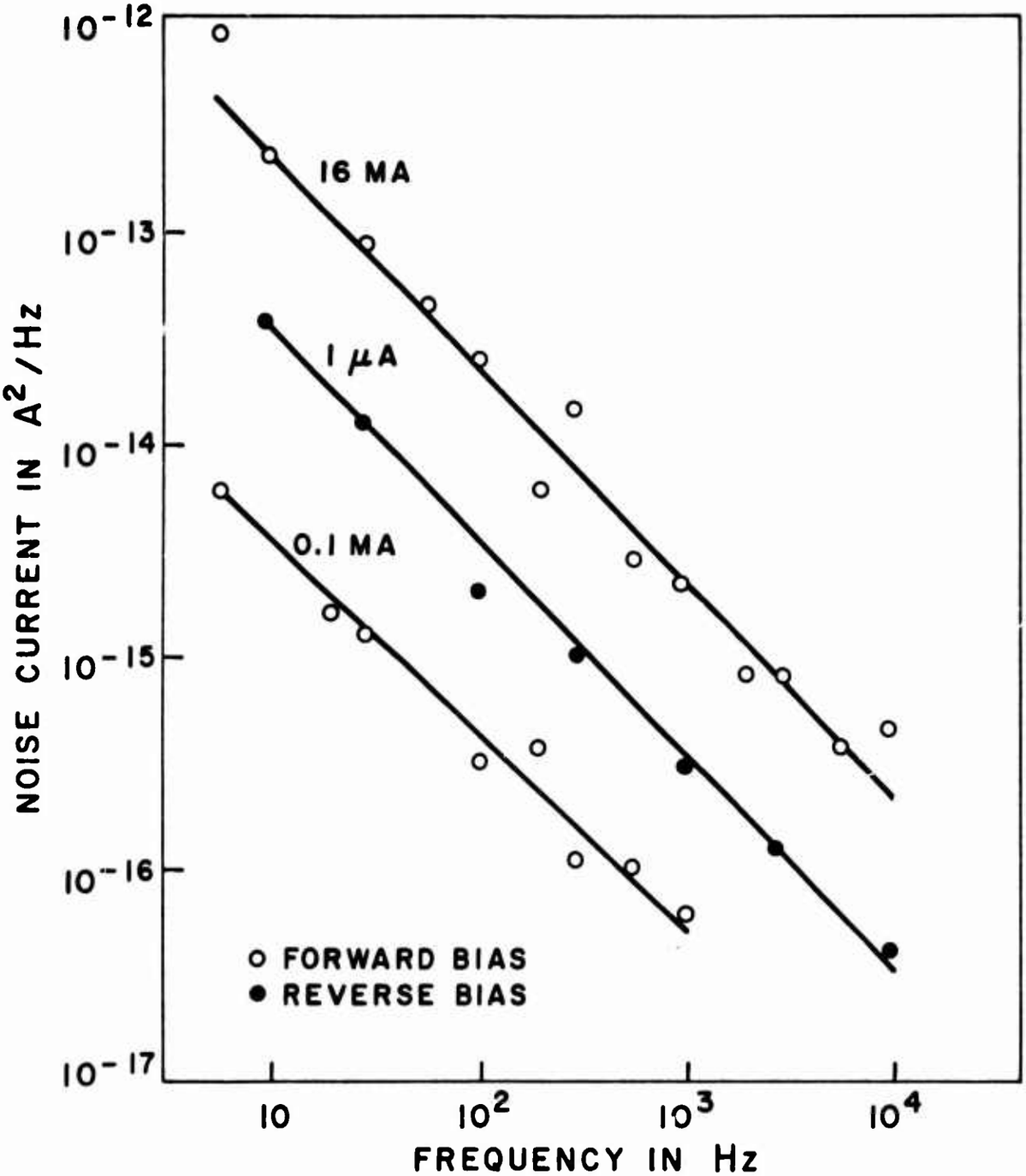

Figure 4. Forward and Reverse Current Noise Spectra of Ga(AsP) Luminescent Diode.

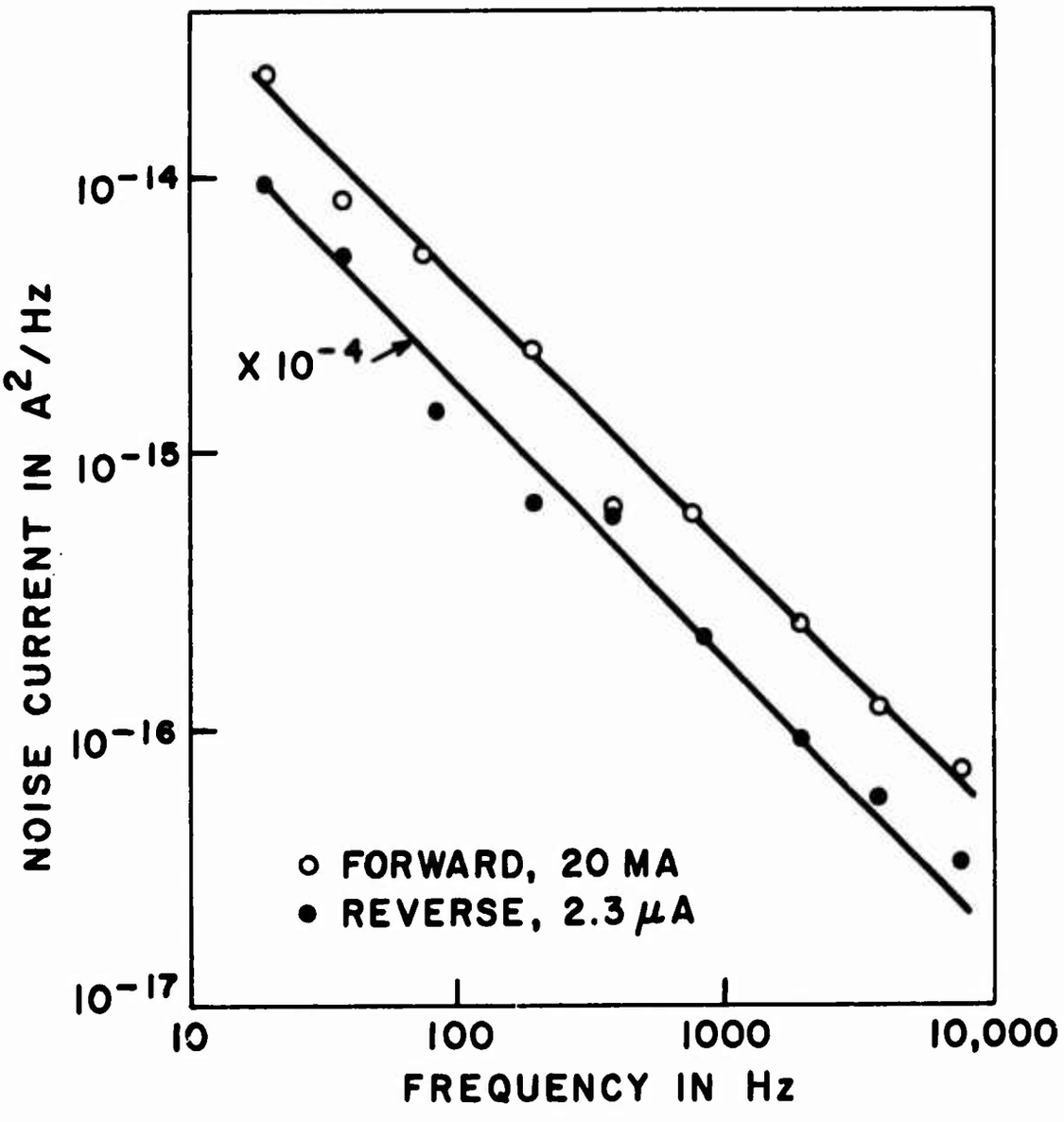

Figure 5. Forward and Reverse Current Noise Spectra of Laser Diode.

The optical emission fluctuation spectrum from the GaAs luminescent diode is shown by the solid data points in Figure 6. Although there is some scatter, the data are consistent with a relaxation time of 12 milliseconds. These results clearly demonstrate that optical fluctuations are present in the luminescent emission. It is interesting to note that other work[10] has not been able to detect such optical fluctuations from laser diodes below the lasing threshold.

Of somewhat greater significance is the noise spectrum resulting from cross-correlation between the junction forward current noise and optical emission fluctuations. This data is shown by open data circles in Figure 6. Here, two relaxation times, 12 and 0.45 milliseconds are visible in the spectrum. This data shows in a most direct way the relation between forward current noise and emission fluctuations. It establishes that the relaxation times can be interpreted in terms of carrier transitions in the junction region.

The above experimental data repeated with tungsten lamp illumination substituted for GaAs emission are given in the lower curve of Figure 6. For these experiments, the lamp intensity was adjusted so that the dc photocurrents were the same as for the diode illumination. Both the optical emission fluctuations and the cross-correlation between diode current noise and tungsten lamp emission noise are at the sensitivity limit of the correlator-amplifier system. That is, no correlated noise signals can be detected when tungsten lamp illumination is present. The indicated noise level in the presence of GaAs radiation is several orders of magnitude greater

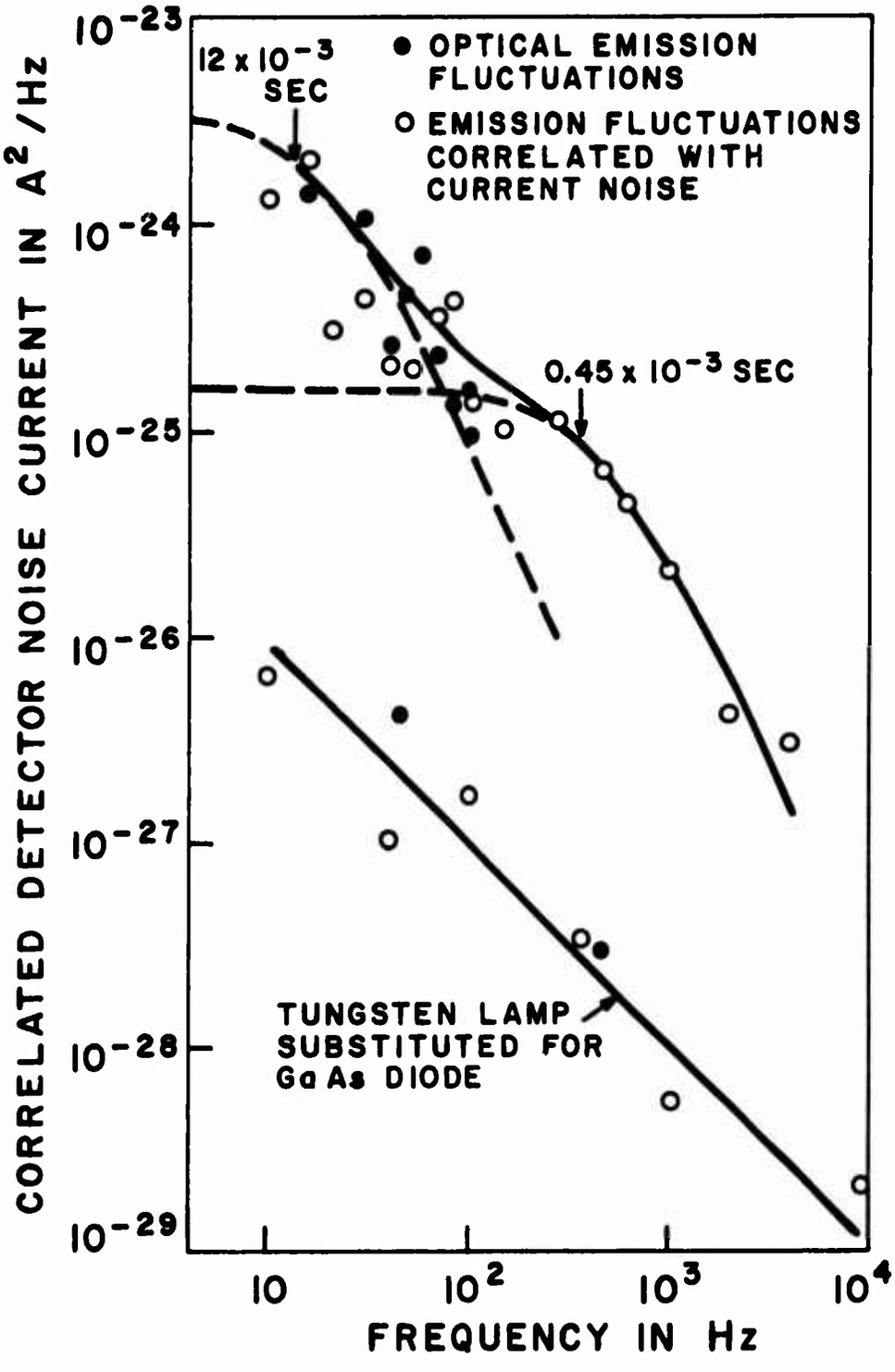

Figure 6. Optical Emission Noise Spectrum and Correlated Optical Emission-Forward Current Noise Spectrum of GaAs Luminescent Diode.

than this limit of sensitivity. These results show that the measured optical noise truly represents emission fluctuations and is not an artifact introduced by the apparatus.

Optical emission fluctuations increase with diode forward current, as illustrated in Figure 7. The current range is rather restricted, being limited at low currents by detector sensitivitv and at high currents by Joule heating of the diode. The data indicate that emission noise increases as the square of the injection current, as expected on the basis of recombination transition fluctuations. Similarly, the correlated noise level increases with the square of the current (solid data points in Figure 7), which is satisfactory confirmation of the optical noise results.

The optical emission noise spectrum of the laser diode shows only 1/f noise, in conformity with the forward current noise results. In addition, the correlation between forward current noise and optical fluctuations, Figure 8, is also a 1/f noise spectrum. The magnitude of the noise is found to increase with the square of the current. It is clear that the source of 1/f noise in the junction current produces similar fluctuations in the optical output. Note also that the noise level in this diode is much larger than in the previous case, suggesting that the 1/f noise masks any effect associated with carrier recombinations at one or two discrete levels.

It was not possible to detect any optical emission fluctuations nor correlation between emission noise and forward current noise in the case of the Ga(AsP) diode. The single-channel optical noise is

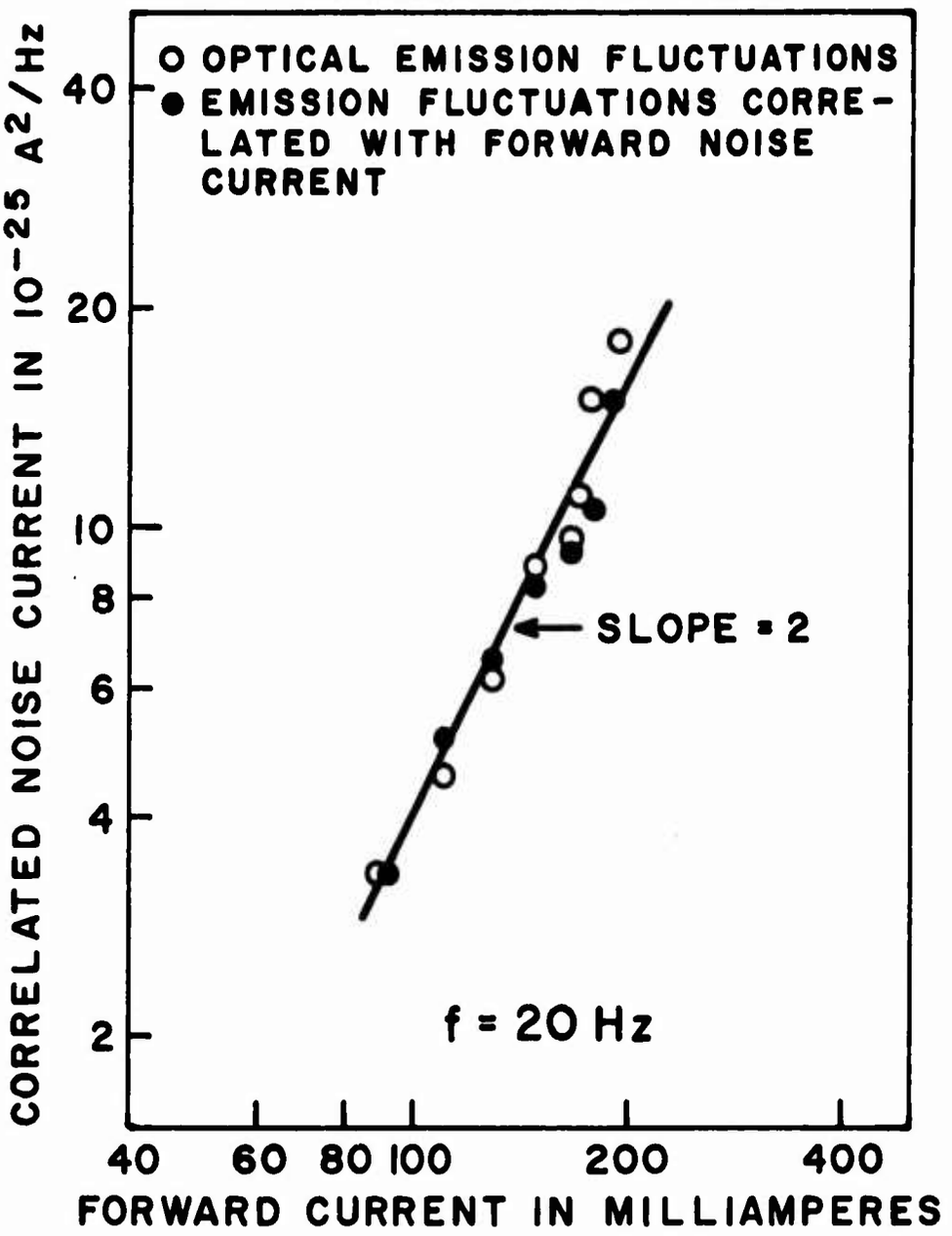

Figure 7. Variation of Optical Emission Fluctuations from GaAs Luminescent Diode with Forward Current.

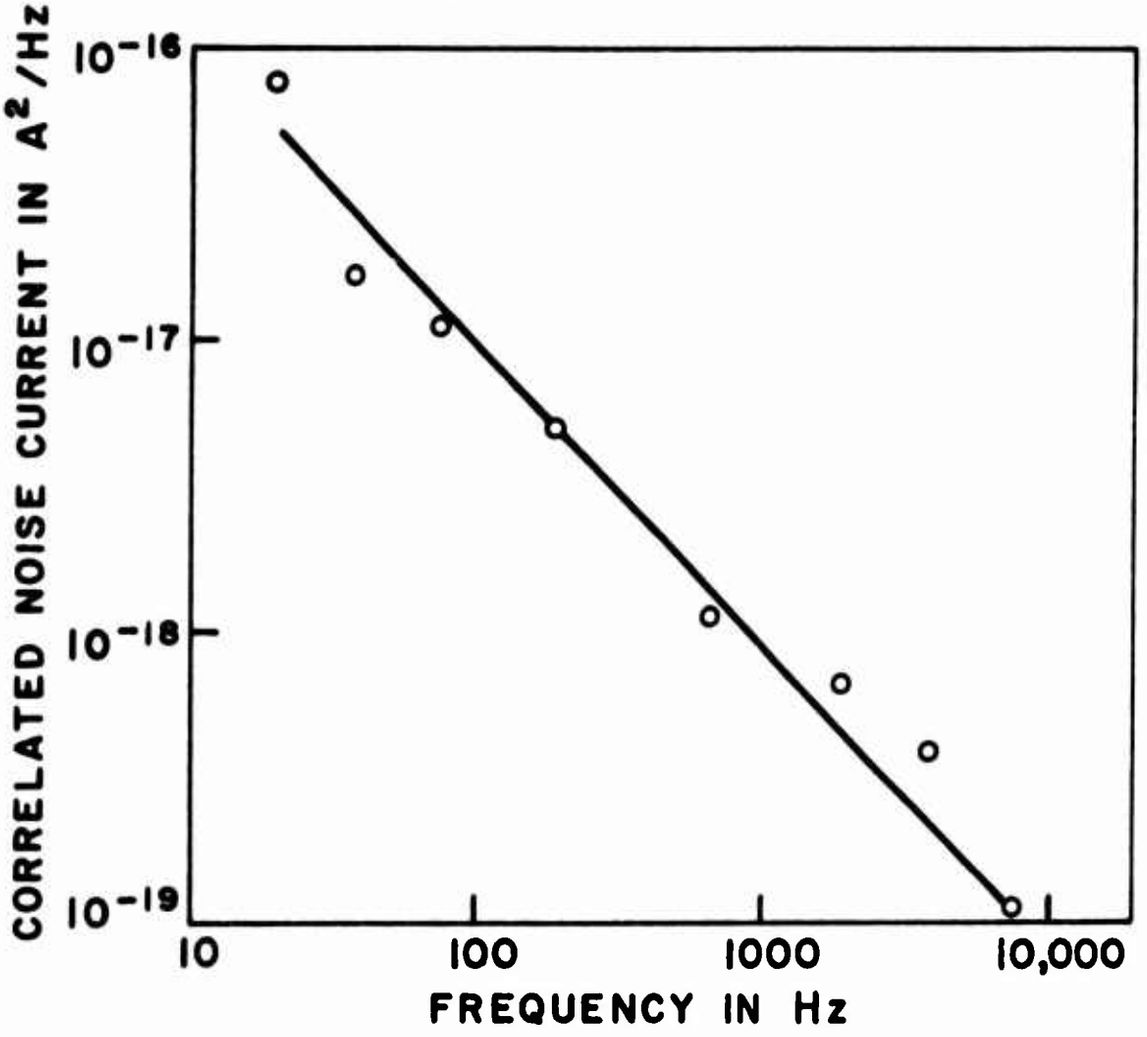

Figure 8. Correlated Optical Emission-Forward Current Noise Spectrum of Laser Diode.

simple white shot noise associated with the photomultiplier anode current. Good quantitative agreement with the predicted shot noise level is observed, confirming that the optical emission fluctuations from this diode are completely random. Both the shot noise magnitude and the optical output (as measured by the photomultiplier anode current) increase approximately with the square of the junction forward current, Figure 9, for small values of current. At higher injection levels, both become a linear function of diode current. Such super-linear behavior has previously been observed in similar electro-luminescent diodes involving indirect transitions.[11]

The junction forward current noise level, also shown in Figure 9, is not a simple function of forward current, either. Conventional square-law behavior is seen at low currents, with a break in the curve at currents of a few milliamperes (forward bias 1.45 to 1.5 volts). The noise spectrum remains 1/f noise both below and above this transition region, as seen in Figure 4. Above this region the noise level appears to be a linear function of current, although the data is limited and it is probable that extending the data to higher currents (not possible because of Joule heating) would establish a square-law trend.

V. DISCUSSION

These measurements establish the existence of optical emission fluctuations from p-n junction luminescent diodes. It appears that emission noise spectra exhibiting discrete characteristic

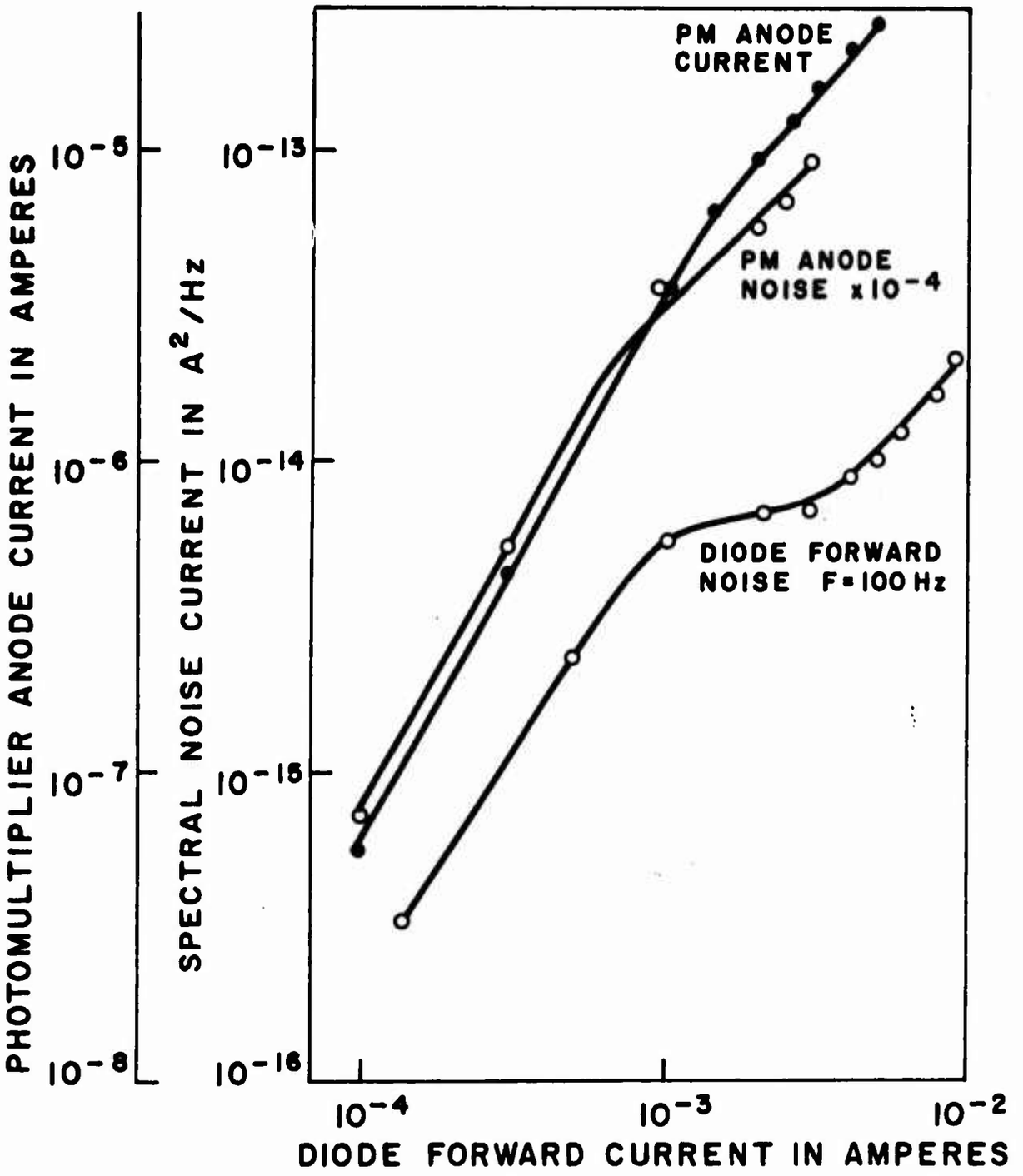

Figure 9. Variation of Luminescent Output, Photon Noise, and Diode Forward Noise with Forward Current for Ga(AsP) Luminescent Diode.

time constants are associated with junctions in which carrier recombination occurs in the space charge region. Other carrier transport properties (e. g., tunneling) may lead to 1/f optical noise spectra. In either case correlation is observed between the forward current noise and the optical emission noise, suggesting that carrier transitions responsible for both phenomena are the same.

It seems likely that the high impurity concentration of the laser diode compared to the GaAs luminescent diode reduces the influence of discrete levels because they merge with the band edges. This, together with the strong 1/f noise level of unknown origin, masks any structure in the noise spectra. Furthermore, if a significant fraction of the diode current is a result of carrier diffusion across the junction, optical emission fluctuations other than photon noise are not present.

The author is grateful to Samuel L. Webb and William D. Brennan for much help and advice in pursuing this work.

REFERENCES

[1] M. D. Montgomery, J. Appl. Phys. 32, 2408 (1961).

[2] F. J. Hyde, Proc. Phys. Soc. B. 69, 231 (1956).

[3] B. V. Rollin and J. P. Russell, Proc. Phys. Soc. 81, 578 (1963); F. M. Klaassen, J. Blok and H. C. Booy, Physica 27, 48 (1961); L. Johnson and H. Levinstein, Phys. Rev. 117, 1191 (1960).

[4] A. G. Jordan and R. W. Knepper, Appl. Phys. Letters 6, 126 (1965).

[5] T. M. Chen and A. van der Ziel, Physica 31, 1632 (1965).

[6] See, for example, J. A. Armstrong and A. W. Smith, Phys. Rev. 140, 155 (1965).

[7] T. N. Morgan, Phys. Rev. 139A, 294 (1965).

[8] J. J. Brophy, M. Epstein and S. L. Webb, Rev. Sci. Instr. 36, 1803 (1965).

[9] D. C. Agouridis and K. M. van Vliet, Proc. IRE 50, 2121 (1962).

[10] J. A. Armstrong, Phys. Rev. Letters 14, 68 (1965).

[11] H. G. Grimmeiss, A. Rabenau and H. Koelmans, J. Appl. Phys. 32, 2123 (1961).

FIGURE CAPTIONS

Figure 1. Electroluminescent Emission and Photoelectric Response Spectra of GaAs, Ga(AsP), and GaAs Laser Diodes.

Figure 2. Block Diagram of Experimental Equipment to Measure Optical Emission Fluctuations of a Luminescent Diode.

Figure 3. Forward and Reverse Current Noise Spectra of GaAs Luminescent Diode.

Figure 4. Forward and Reverse Current Noise Spectra of Ga(AsP) Luminescent Diode.

Figure 5. Forward and Reverse Current Noise Spectra of Laser Diode.

Figure 6. Optical Emission Noise Spectrum and Correlated Optical Emission-Forward Current Noise Spectrum of GaAs Luminescent Diode.

Figure 7. Variation of Optical Emission Fluctuations from GaAs Luminescent Diode with Forward Current.

Figure 8. Correlated Optical Emission-Forward Current Noise Spectrum of Laser Diode.

Figure 9. Variation of Luminescent Output, Photon Noise, and Diode Forward Noise with Forward Current for Ga(AsP) Luminescent Diode.

APPENDIX II

MEASUREMENTS ON SEMICONDUCTOR PN JUNCTIONS

by

James J. Brophy and Samuel L. Webb

IIT RESEARCH INSTITUTE

MEASUREMENTS ON SEMICONDUCTOR PN JUNCTIONS

by

James J. Brophy and Samuel L. Webb
IIT Research Institute
Chicago, Illinois 60616

ABSTRACT

The semiconductor p-n junction is an ideal subject for laboratory experiments because of its wide range of interesting and useful properties. Furthermore, agreement between experimental results and simple semiconductor theory is most satisfying. Studies of injection luminescent diodes allow optical investigations to be included along with the usual electrical measurements. It is possible to determine essentially all of the important properties of a p-n junction, such as junction area, width, internal potential, saturation current, impurity content, etc., by straightforward non-destructive measurements. Furthermore, the properties which are important in practical semiconductor devices are made apparent.

I. INTRODUCTION

Of all the many useful solid state devices, the semiconductor p-n junction is most notable on at least two counts: the number and variety of properties which find practical application, and the good agreement between experimental measurements and simple theoretical concepts. The various forms of p-n junctions are useful as rectifiers, voltage regulators, variable capacitors, photocells, nuclear radiation detectors, photoelectric generators, light sources, lasers, etc. In each case the desirable property is explicable in terms of simple semiconductor physics and quantitative agreement with experimental results is most gratifying. Detailed study of semiconductor p-n junctions is therefore very appropriate for beginners in semiconductor physics and solid state electronics. Furthermore, the p-n junction is the basis for many other semiconductor devices such as the transistor.

Recently, p-n junctions producing visible and infrared radiation have become available at modest prices. This adds optical measurements to the broad scope of electrical measurements that can be made on the same device and greatly expands the pedalogical usefulness of laboratory experiments designed to demonstrate semiconductor behavior. Since a wide range of properties can be examined on the same unit, it is possible to demonstrate how each property can be emphasized by suitable adjustment of junction parameters.

This paper reports the results of such measurements carried out on commercially available injection luminescent diodes and shows

how each piece of data is interpretable in terms of simple semiconductor physics. Although the main purpose is to demonstrate typical data which should be useful in design of laboratory experiments, these collected results also show how a series of measurements can be used to discover important junction parameters. It proves possible to determine essentially all of the important parameters of the junction, with the exception of chemical identification of the p-type and n-type impurities, by reproducible, nondestructive measurements.

The particular units examined here are a type GAE-402 gallium arsenide infrared-emitting junction obtainable from Philco Corporation and a mixed-crystal gallium arsenide-gallium phosphide diode which emits in the visible red region, obtainable from Monsanto Company. Equally suitable diodes are easily available from other sources such as radio parts supply companies.

II. CURRENT-VOLTAGE CHARACTERISTIC

The current-voltage characteristic of an ideal p-n junction is given by the rectifier equation[1]

$$I = I_o(e^{eV/kT} - 1) \qquad (1)$$

where I is the current, V is the applied voltage, e is the electronic charge, k is Boltzmann's constant and I_o is the reverse saturation

current. The quantity I_o can be expressed in terms of basic semiconductor parameters but the reverse current of practical semiconductor devices is dominated by surface leakage. The importance of surface leakage is demonstrated when the true bulk saturation current is determined in a later section.

Equation (1) is a good representation of experimental results, Figure 1, until reverse-bias breakdown occurs. In particular, the excellent rectification ratio of p-n junctions is immediately apparent in Equation (1) and the experimental data. The forward-bias offset voltage, also apparent in Figure 1, is a consequence of the vastly different values of reverse saturation current in the two semiconductor materials. This difference may be related directly[2] to the forbidden energy gaps, which are 1.4 eV in the case of GaAs and 1.97 eV for the particular Ga(AsP) device investigated here. Equation (1) may be used in connection with the experimental data to estimate the ratio of reverse saturation currents of the two diodes by noting the forward biases required to produce the same forward current; the result, 2.4×10^7, will be compared with a more direct measurement below.

Actually, semilog plots of the experimental forward characteristics reveals that the slopes are smaller than the value e/kT predicted by Equation (1). This is a consequence of carrier recombination in the junction region[3] and is to be expected for electroluminescent diodes in which just such recombination, in fact, leads to

photon emission.[4] Conventionally, the slope is represented by $e/\beta kT$, where the parameter β is unity in the absence of such recombination and equal to 2 when recombination dominates. These experimental data yield $\beta = 1.9$ for the GaAs diode and $\beta = 1.5$ for the Ga(AsP) diode. This suggests that recombination in the junction region dominates in the GaAs unit while significant carrier diffusion across the junction is present in the latter device.

III. AVALANCHE BREAKDOWN

At a critical reverse bias potential, the electric field in the junction accelerates carriers sufficiently to produce new carriers by collisional ionization of neutral atoms. These additional carriers are similarly accelerated and generate more carriers. The result is a rapid increase in reverse current at the critical reverse bias, which is called avalanche breakdown. This effect is quite similar to a Townsend discharge in gases and may be treated in the same manner.[5]

Avalanche breakdown is clearly evident in Figure 1 for both diodes. The critical potential is about 4 volts for the GaAs diode, although the breakdown is rather "soft." The transition is much more rapid in the case of the Ga(AsP) unit, and occurs at 7.5 volts. This property is emphasized in zener diodes, which are used as voltage regulators, in order to keep the terminal voltage constant over as wide a current range as possible.

The critical voltage at which avalanche breakdown is initiated depends upon the width of the junction, which is controlled by the impurity content of the semiconductor (see Section IV). Published data[6] may be used to determine the impurity content from the observed breakdown voltage. The result is 1×10^{18} and 4×10^{17} impurities/cm^3 for the GaAs and Ga(AsP) units, respectively. In addition, the critical field in the junction can be calculated once the junction width is determined (next section). The breakdown field is 5×10^5 v/cm for both units.

IV. JUNCTION CAPACITANCE

A p-n junction is two layers of opposite charge separated by the width of the junction and so has the properties of electrical capacitance. The junction width is a function of applied voltage, however, so the capacitance of the junction is electrically variable. In the case of an abrupt junction (the transition from p-type to n-type impurities occurs over a very short distance in the crystal), and when one side has a much greater impurity content then the other, the junction capacitance obeys the relation[7]

$$\frac{1}{C^2} = \frac{2}{\epsilon_o K_e e N A^2} (V_o + V) \qquad (2)$$

where ϵ_o is the permitivity of free space, K_e is the dielectric constant, N is the impurity content of the lightly-doped region, A is

the area of the junction, and V_o is the internal potential rise at the junction.

Experimental results for both diodes are in agreement with Equation (2) as shown in Figure 2. This confirms that both are abrupt junctions, for otherwise the data would not plot as straight lines. The intersection of the lines with the abscissa determines the built-in potential difference V_o between the n-type and p-type regions. This is perhaps the most straightforward experimental technique for demonstrating the existence of this rather elusive quantity.

The junction area is calculated from the slope of the lines in Figure 2 using the value for N determined from reverse breakdown and taking the dielectric constant for GaAs, 12.5, to be appropriate for the other semiconductor as well.[8] The areas are both of the order of 10^{-3} cm^2, which is in good agreement with manufacturers' data.

The junction width may be determined from the expression for the capacitance of a parallel-plate capacitor,

$$d = \frac{\epsilon_o K_e A}{C} \qquad (3)$$

Inserting measured values, the width is 370 Å (GaAs diode) and 590 Å (Ga(AsP) diode) at zero applied voltage. The widths increase to 730 Å and 1700 Å, respectively, at potentials corresponding to

avalanche breakdown. These values are used to calculate the breakdown field in the previous section.

V. PHOTOELECTRIC RESPONSE

A reverse-biased p-n junction is a sensitive radiation detector because the minute reverse saturation current (in the dark) is enhanced significantly by generation of hole-electron pairs near the junction by absorbed photons. The wavelength response of such a photocell is sharply peaked at photon energies corresponding to the forbidden energy gap. This is so because less energetic photons have insufficient energy to excite electrons across the gap and more energetic photons are absorbed so near the surface that carriers do not reach the junction.

On this basis, the forbidden energy gaps of the two semiconductor materials are 1.39 eV and 1.97 eV, as illustrated in Figure 3. Actually, this interpretation must be used with some caution in such heavily doped materials as used here because of the possibility of impurity banding, but this introduces only a small error in any event. Note that the internal potential rises determined earlier are consistent with these values of forbidden energy gaps.

VI. INJECTION ELECTROLUMINESCENCE

Under forward bias the recombination of some injected electrons and holes is accompanied by the creation of photons. The

energy of the emitted photon is approximately equal to the width of the forbidden energy gap since this represents the energy difference between free carriers on the opposite sides of the junction.

Experimental data, Figure 3, shows that the maximum emission in both diodes, 1.35 eV and 1.91 eV, respectively, occurs at somewhat longer wavelengths than those corresponding to the forbidden energy gaps. This suggests that recombination takes place at impurity centers located near (approximately 0.05 eV) to one of the band edges. This interpretation is consistent with the values of β found earlier since recombination at impurity sites would most likely lead to recombination within the junction region.

Using published data,[9] the emission peak at 1.91 eV establishes that the mixed crystal Ga(AsP) diode is fabricated from a material which contains a 60/40 arsenic/phosphorous ratio. Similar information could be obtained from the width of the forbidden energy gap as established by the photoelectric response, since the width of the gap is known to be a continuous function of the relative GaAs-GaP composition.

It is interesting that the energy of emitted photons is greater than the applied forward bias (compare Figure 1 and Figure 3). The energy difference is supplied by thermal energy of the crystal, which means that the diode is cooled by this electroluminescent refrigeration.[10] Each photon carries away a significant amount of energy and appreciable cooling can be obtained in principle. The efficiency is drastically impaired, however, by internal reabsorption,

surface reflection losses, and the fact that only a small fraction of injected carriers recombine with photon emission.

VII. PHOTOELECTRIC GENERATION

As a consequence of the internal potential rise at a p-n junction, optically generated carriers are collected at the junction and tend to bias it in the forward direction. The junction thus becomes a photoelectric generator, an effect used in the familiar silicon solar cell. The current-voltage characteristic of the cell is written as[11]

$$V_L = \frac{kT}{e} \ln\left(1 + \frac{I_g - I_L}{I_o}\right) - R I_L \qquad (4)$$

where V_L and I_L are the voltage and current of the load connected to the cell, I_g is the current corresponding to collected holes and electrons created by photon absorption, and R_L is an effective internal series resistance.

Experimental data corresponding to Equation (4) are illustrated in Figure 4 with the diodes exposed to tungsten illumination. Values for the unknown quantitites in Equation (4) are determined by fitting the expression to the experimental data at the two intercepts and at a data point in between. The result yields true values for I_o (2.4×10^{-16} and 6.6×10^{-24} amp) which are many

orders of magnitude smaller than observed in the current-voltage characteristic, Figure 1. As mentioned previously, the difference is attributable to surface leakage in the latter measurement. The ratio of the true saturation currents as determined from the photoelectric generator approach is 3.6×10^7, which is in good agreement with the previous value calculated from the forward characteristic.

An estimate of the potential conversion efficiency can be obtained by calculating the maximum electrical power output from Figure 4 and comparing this with the input power, assuming all photons have energies corresponding to the peak of the photoelectric response, Figure 3. The result is 24 percent and 29 percent for the GaAs and Ga(AsP) diodes, respectively. This is not a practical efficiency, of course, since it does not account for reflection losses and non-spectral incident illumination. Nevertheless, values of the order of 25 percent can be calculated (on the same basis) for practical silicon solar cells.

VIII. SUMMARY

The combination of these measurements illustrates how it is possible to determine the forbidden energy gap, impurity concentration and composition (in the case of mixed crystals) of semiconductors used to fabricate p-n junctions using non-destructive means. The junction area, width, internal potential rise, and saturation current are similarly determined. Furthermore, the junction can be shown to be abrupt and that appreciable carrier recombination occurs

in the junction region. Thus, except for the chemical identification of impurities, essentially all of the important properties of a p-n junction are established.

Each measurement also illustrates an important property of the p-n junction which finds application in a practical semiconductor device. The factors which maximize a selected property for practical application are quite apparent in each case. This makes such investigations appropriate for those interested in semiconductor electronics as well as in semiconductor physics.

REFERENCES

[1] L. V. Azaroff and J. J. Brophy, Electronic Processes in Materials, (McGraw-Hill Book Co., Inc., New York, 1963), p. 274.

[2] ibid., p. 276.

[3] C. T. Sah, et al., Proc. IRE 45, 1228 (1957).

[4] T. N. Morgan, Phys. Rev. 139A, 294 (1965); D. F. Nelson, Phys. Rev. 149, 574 (1966).

[5] J. Yamashita, Progress in Semiconductors, Vol. 4, A. F. Gibson, ed., (John Wiley & Sons, Inc., New York, 1960).

[6] M. Weinstein and A. I. Mlavsky, Appl. Phys. Letters 2, 97 (1963).

[7] see Reference 1, p. 277.

[8] C. Hilsum, Progress in Semiconductors, Vol. 9, A. F. Gibson and R. E. Burgess, eds., (Temple Press Books, Ltd., London, 1965).

[9] D. A. Cusano, G. E. Fenner and R. D. Carlson, Appl. Phys. Letters 5, 144 (1964).

[10] G. C. Dousmanis, C. W. Mueller, H. Nelson and K. G. Petzinger, Phys. Rev. 133, A316 (1964).

[11] see Reference 1, p. 282.

FIGURE CAPTIONS

Figure 1. Current-Voltage Characteristics of GaAs and Ga(AsP) Diodes.

Figure 2. Variation of Junction Capacitance with Reverse Bias.

Figure 3. Electroluminescent Emission and Photoelectric Response Spectra of GaAs and Ga(AsP) Diodes.

Figure 4. Output Characteristics of GaAs and Ga(AsP) Diodes Under Tungsten Lamp Illumination. Data Points are Experimental and Solid Curves are Theoretical.

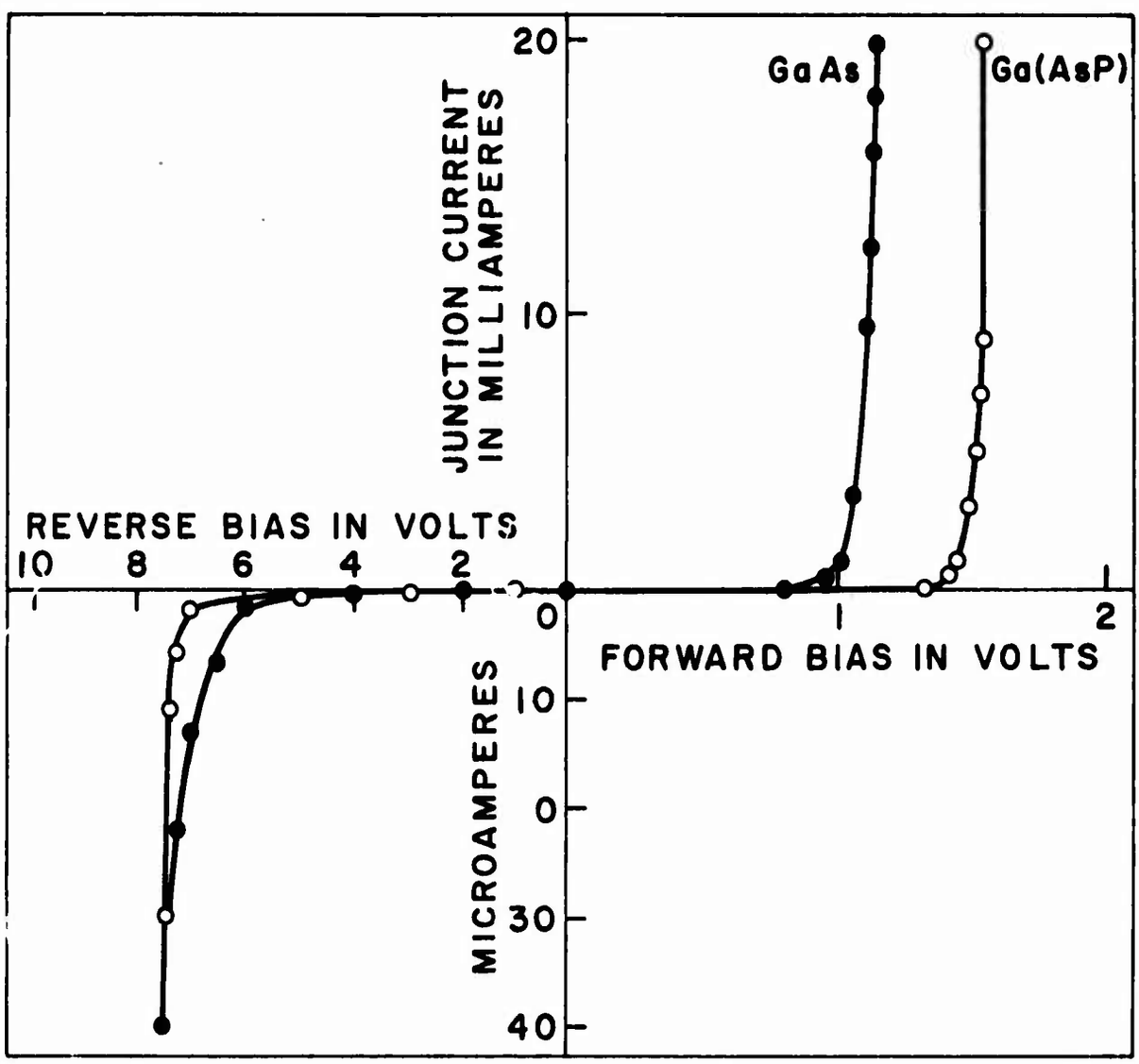

Figure 1. Current-Voltage Characteristics of GaAs and Ga(AsP) Diodes.

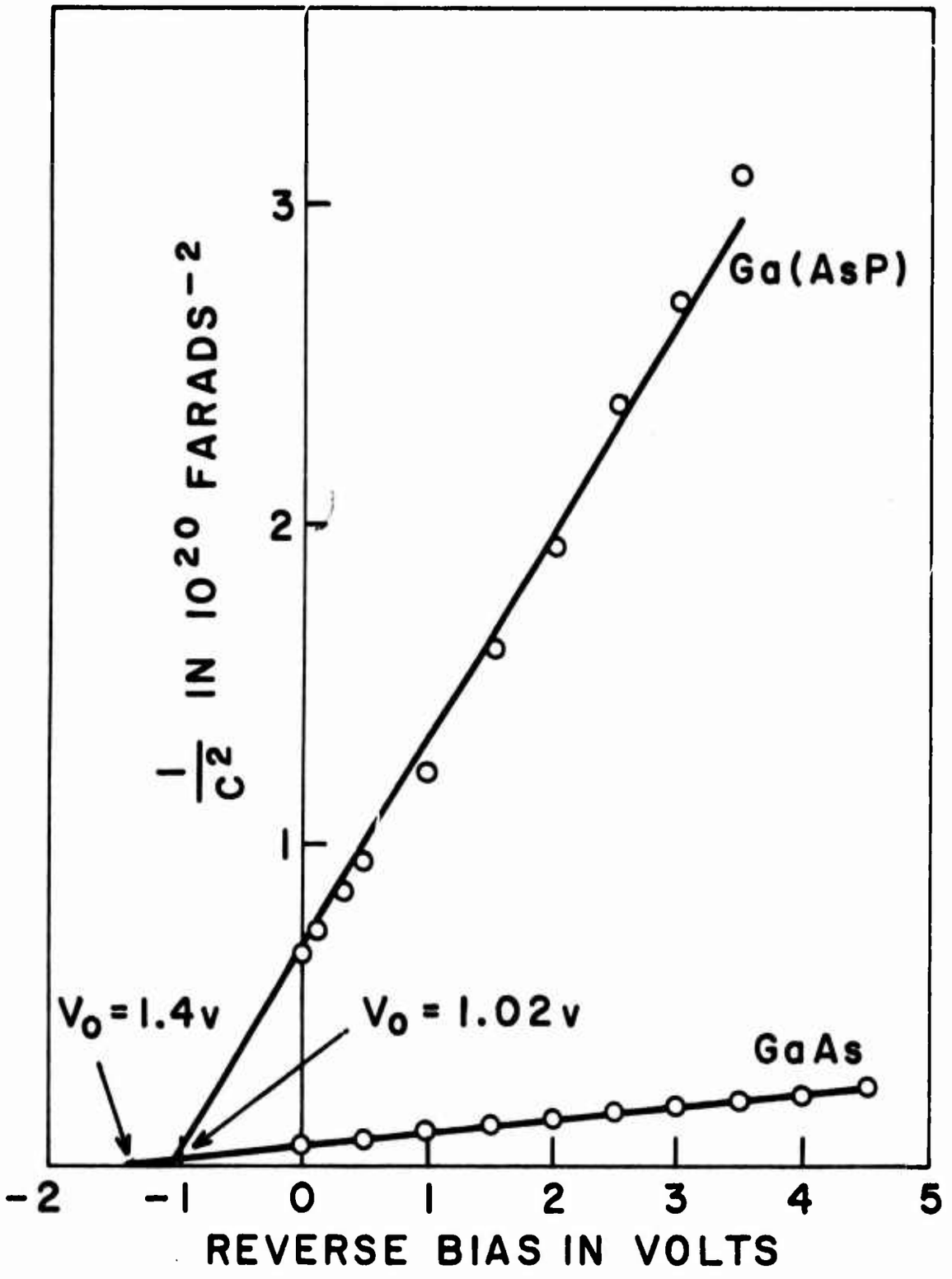

Figure 2. Variation of Junction Capacitance with Reverse Bias.

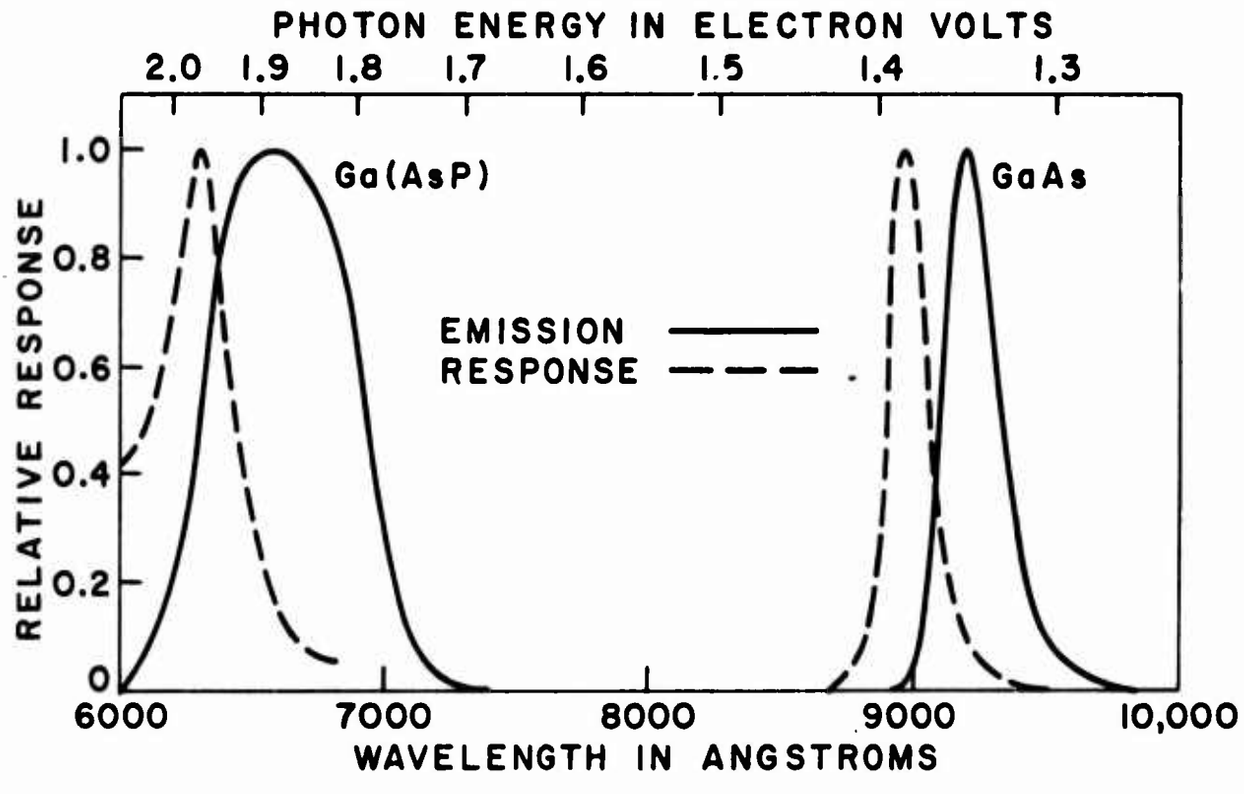

Figure 3. Electroluminescent Emission and Photoelectric Response Spectra of GaAs and Ga(AsP) Diodes.

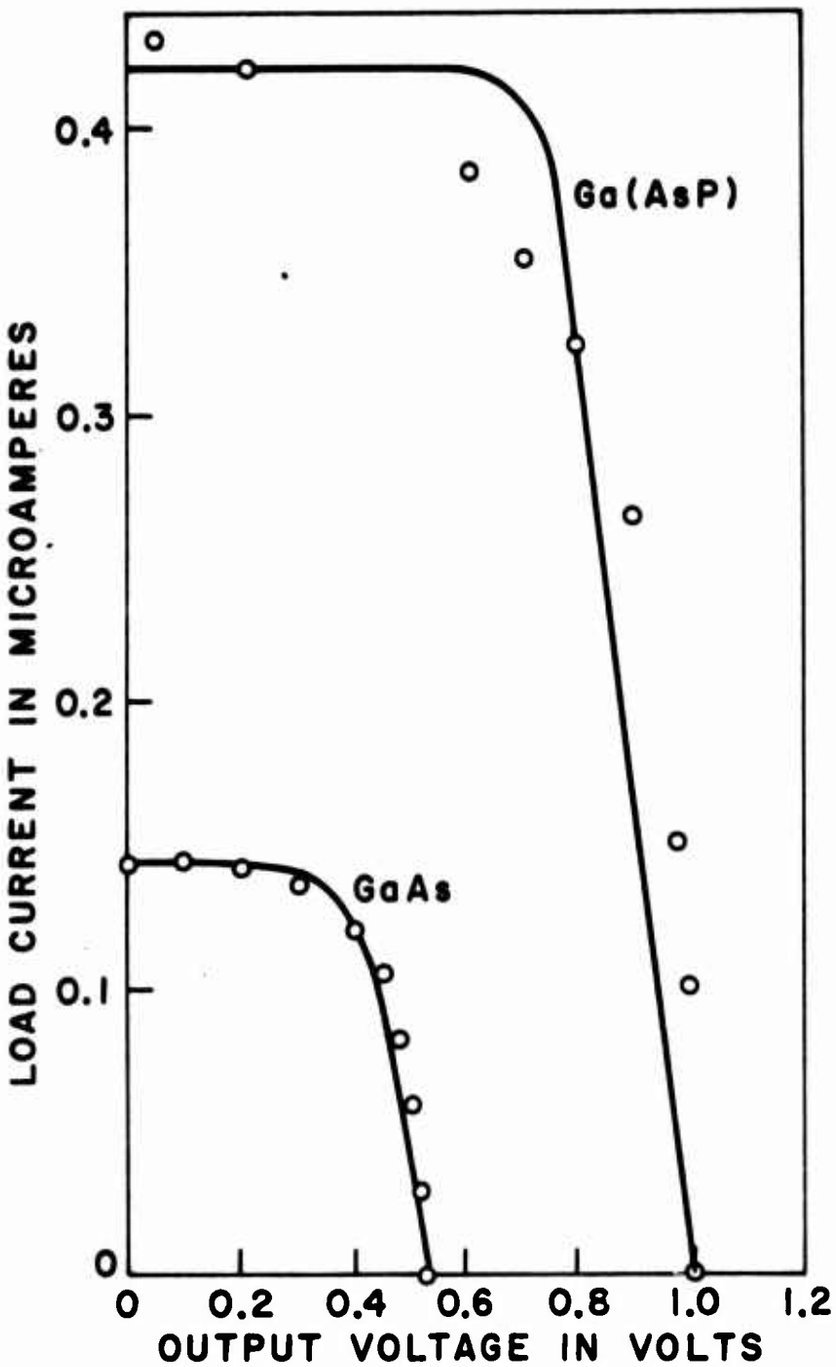

Figure 4. Output Characteristics of GaAs and Ga(AsP) Diodes Under Tungsten Lamp Illumination. Data Points are Experimental and Solid Curves are Theoretical.

APPENDIX III

PHOTOMULTIPLIER TUBE NOISE

by

James J. Brophy

IIT RESEARCH INSTITUTE

APPENDIX III

PHOTOMULTIPLIER TUBE NOISE

In the study of optical emission fluctuations from semiconductors, photomultiplier tubes are used as detectors. It is necessary to check the noise and response properties of the photomultiplier tubes themselves in order to ensure reliable experimental measurements. The noise properties of photomultipliers are quite well established and the experimental measurements can be used to confirm satisfactory operation of the system. This is particularly important in the present experimental work since the photomultipliers are used under somewhat non-standard conditions.

The circuit diagram used in this investigation is shown in Figure 1. The circuit is rather conventional except for the rather high load resistance used to increase the sensitivity at low light levels. Batteries are used in order to minimize extraneous noise effects.

The output noise spectrum in the dark and with the filtered tungsten lamp illumination on the cathode is shown in Figure 2. An optical filter in front of the tungsten lamp permits only wavelengths of the order of 6500 Å to reach the detector. It is apparent that the photomultiplier noise is white noise over the frequency range of interest. Of particular note is the absence of low frequency 1/f

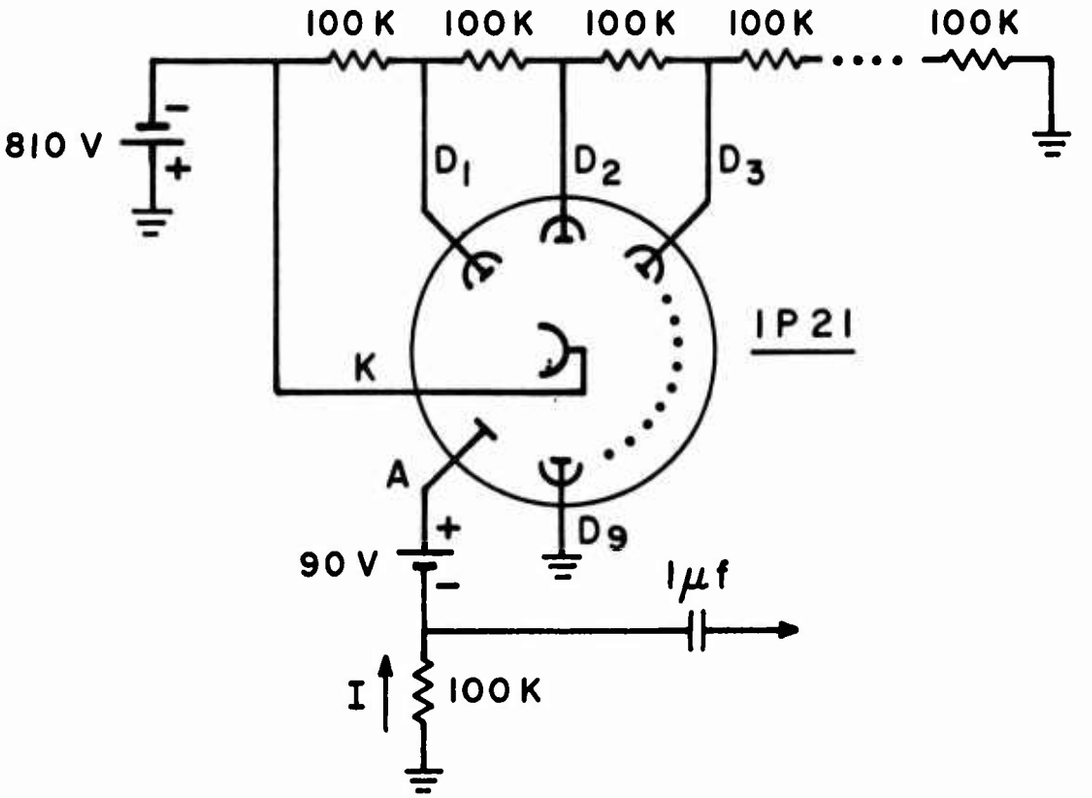

Figure 1. Circuit Diagram of Photomultiplier Tube.

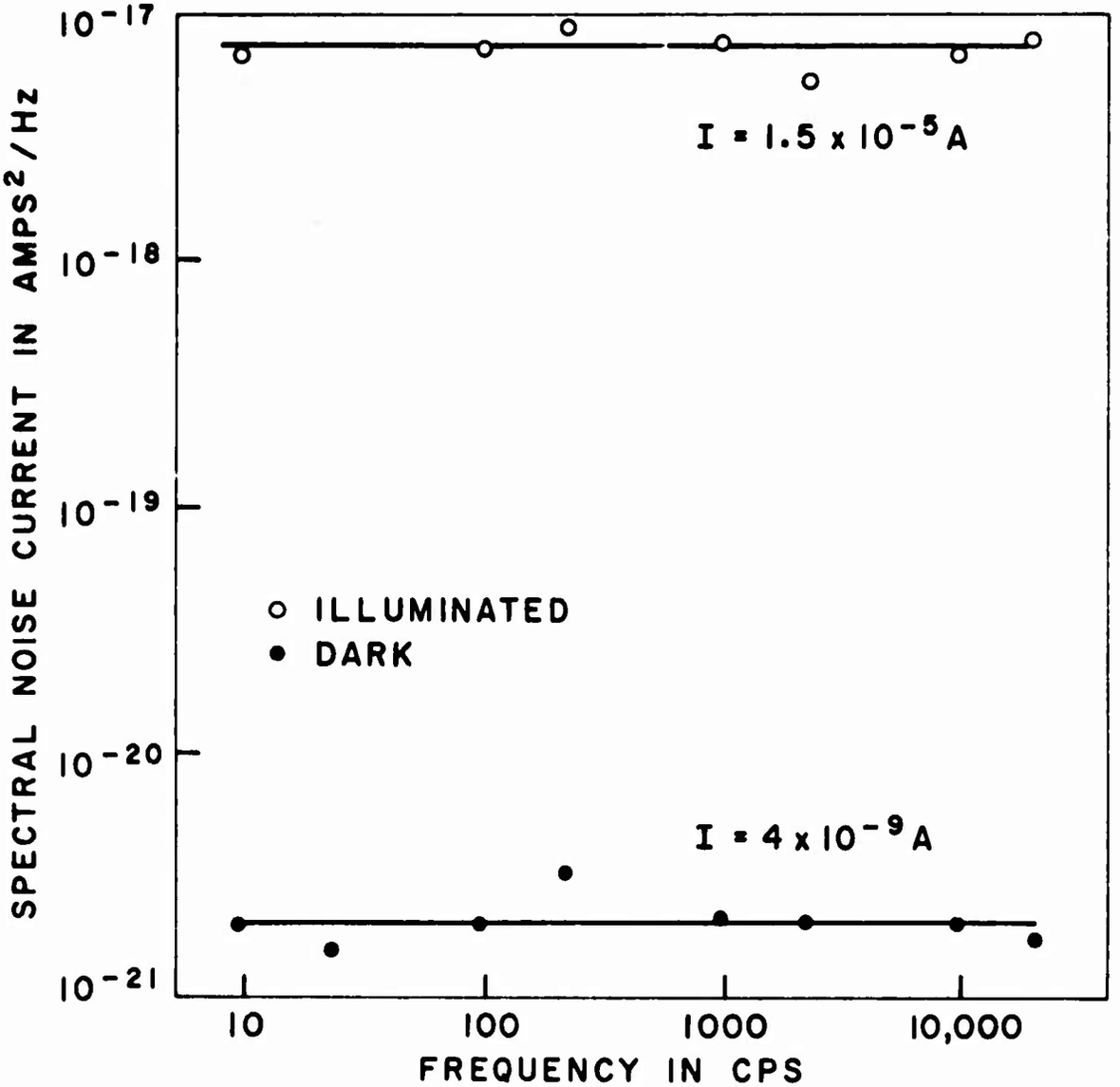

Figure 2. Current Noise Spectra of 1P21 Photomultiplier in the Dark and Under Illumination.

noise effects. This is a desirable feature characteristic of photomultipliers.

The output noise level increases linearly with current as shown in Figure 3. It is satisfying that this behavior persists down to the low illumination levels and anode currents used in this work.

It is well established that photomultiplier tube noise is a result of shot noise of photoelectric emission current from the cathode amplified by secondary emission multiplication.[1] This simple shot noise level is modified by the statistical properties of secondary emission so that the mean square anode noise current is given by

$$\langle \Delta i^2 \rangle = 2eI \left(\delta^n \frac{H - 1}{\delta - 1} \right) , \qquad (1)$$

where $\langle \Delta i^2 \rangle$ and I are the mean square and average anode current, δ is the secondary emission ratio, and H accounts for the statistical nature of the secondary emission process; it is a measure of the departure from the average number of secondary electrons per primary. The quantity δ^n is the overall gain of the photomultiplier.

According to Equation (1), the anode noise is independent of frequency and increases linearly with current as illustrated by the experimental measurements in Figures 2 and 3. Inserting experimental

[1] A. van der Ziel, Noise (Prentice-Hall, Inc., Englewood Cliffs, N. J., 1956), p. 116.

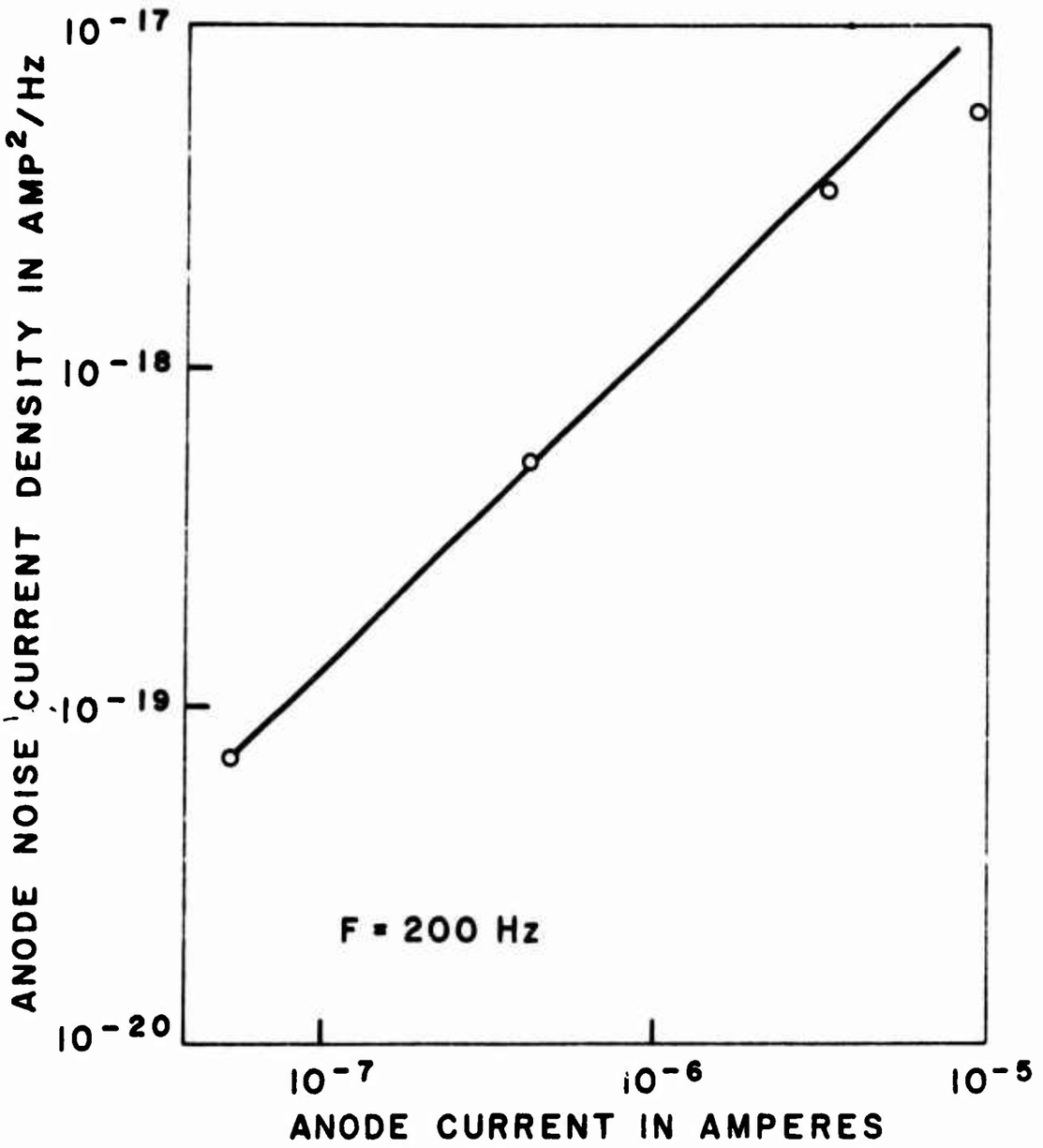

Figure 3. Variation of IP21 Anode Noise with Anode Current

values for the measured noise and anode current and using the tabulated value for the gain, it is possible to calculate the secondary emission ratio and the statistical parameter, H:

	$\langle \Delta i^2 \rangle$ amp^2/Hz	I amp	$\delta^n \frac{H-1}{\delta-1}$	δ^n	δ	H
dark	2×10^{-21}	4×10^{-9}	1.56×10^6	10^6	4.7	6.8
light	7.5×10^{-18}	1.5×10^{-5}	1.56×10^6	10^6	4.7	6.8

These results are in good agreement with published figures.[1]

In order to check the linearity of the anode current-light intensity relationship at low cathode illuminations, a simple inverse square law experiment was carried out. The results in Figure 4 show satisfactory behavior.

These simple experimental measurements indicate that the photomultiplier tubes used in this investigation perform satisfactorily. The noise properties can be explained by simple shot noise and quantitative agreement with previous results is good. It is interesting to note that noise measurements provide a convenient way for checking the secondary multiplication gain of a photomultiplier.

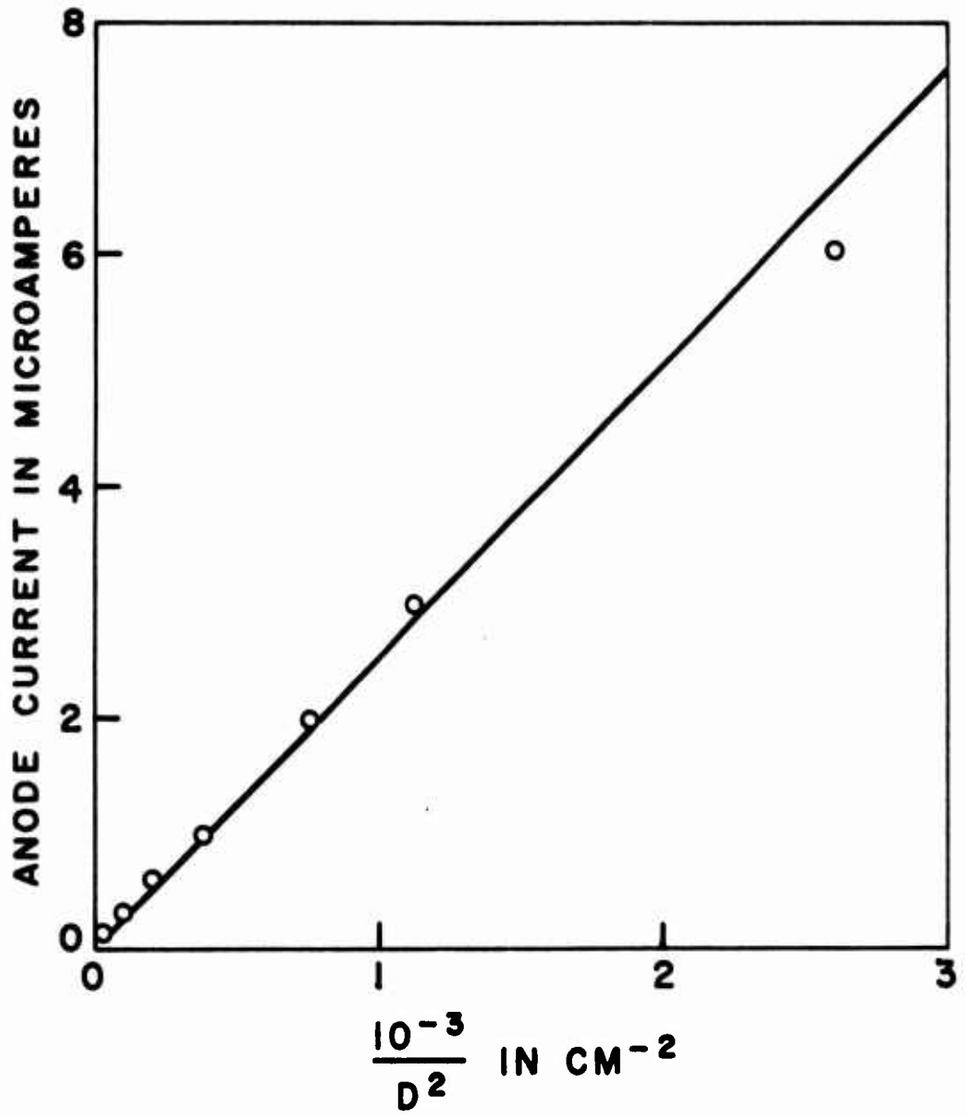

Figure 4. Linearity Check of 1P21 Photomultiplier at Small Anode Currents Using Inverse-Square Law.

APPENDIX IV

CALCULATION OF FLUCTUATIONS IN OPTICAL ABSORPTION

by

Harold N. Spector

APPENDIX IV

CALCULATION OF FLUCTUATIONS IN OPTICAL ABSORPTION

In a previous report,[1] the fluctuations in the optical absorption were related to the noise fluctuations in semiconducting germanium. The optical absorption in this case arises from free carrier absorption and the fluctuations arise from the fluctuations in carrier density. The previous calculation assumed that the carrier density is uniform across the sample and that the fluctuations are correlated throughout the crystal. This latter condition is not valid since, in general, the density fluctuations are only correlated within approximately one diffusion length. The diffusion length in germanium is $d = 2.82 \times 10^{-2}$ cm compared to a sample length of $\ell = 5$ cm. Therefore, the distance in which the fluctuations are correlated is much smaller than the sample length.

Here we will assume that the fluctuations are correlated only within a diffusion length. We divide the sample into $N = \ell/d$ segments and we get for the fluctuations in intensity across each segment,

$$\Delta I_i = -I_T kd \Delta n_i \qquad I_T = I_o e^{-knd} . \tag{1}$$

We have assumed that $k \Delta n_i d \ll 1$ and that the attenuation across the sample is small so that we can assume that the intensity

[1] Annual Summary Report No. 8, Contract No. NOnr 1800(00), November, 1963.

transmitted through each segment, I_T the same for every segment. Summing over all the segments, we obtain

$$\left(\frac{\Delta I}{I_T}\right)^2 = \sum_i \left(\frac{\Delta I_i}{I_T}\right)^2 = (kd)^2 \sum_i (\Delta n_i)^2 = (kd)^2 (\overline{\Delta n})^2 \tag{2a}$$

where

$$(\overline{\Delta n})^2 = \sum_i (\Delta n_i)^2 \ . \tag{2b}$$

This is down by a factor of $(d/\ell)^2$ from the answer obtained assuming the fluctuations are correlated across the sample. Therefore, the fluctuations in intensity should be much smaller than that predicted by the previous analysis.

The fluctuations in intensity can be related to the fluctuations in voltage. Assuming again that the fluctuations are only correlated within a diffusion length, we find for a segment of dimensions d that

$$\Delta V_i = -\frac{I}{d\sigma_o} \frac{\Delta n_i}{n} \ . \tag{3}$$

The mean square voltage fluctuation across the sample is

$$(\Delta V)^2 = \sum_i (\Delta V_i)^2 = \frac{I^2}{(d\sigma_o)^2} \sum_i \frac{(\Delta n_i)^2}{n^2} = \left(\frac{I}{d\sigma_o}\right)^2 \frac{(\overline{\Delta n})^2}{n^2} \tag{4}$$

The voltage across the sample is

$$V = \frac{\ell I}{A\sigma_o} \tag{5}$$

where A is the cross sectional area of the sample. Therefore, we have for the voltage fluctuations, the following expression

$$\frac{(\Delta V)^2}{V^2} = \left(\frac{A}{\ell d}\right)^2 \frac{(\overline{\Delta n})^2}{n^2} \tag{6}$$

The relation between the intensity fluctuations and the voltage fluctuations can be obtained from Equations (2a) and (6),

$$\frac{(\Delta I)^2}{I_T^2} = (knd)^2 \left(\frac{\ell d}{A}\right)^2 \frac{(\Delta V)^2}{V^2} \tag{7}$$

In the previous report it was shown that the following relation between the signal to noise ratio in the detector circuit and $(\Delta I)^2/I_T^2$ holds

$$\frac{S}{N} = \frac{\eta J}{4} \frac{(\Delta I)^2}{I_T^2} . \tag{8}$$

In Equation (8) η is the effective quantum efficiency (given as 0.65) and J is the average transmitted intensity in photons per second. Using Equation (7) in Equation (8), we obtain for the signal-to-noise ratio in terms of the voltage fluctuations

$$\frac{S}{N} = \frac{\eta J}{4} (knd)^2 \left(\frac{\ell d}{A} \right)^2 \frac{(\Delta V)^2}{V^2} \qquad (9)$$

This expression differs by the factor $(\ell d/A)^2$ from the one developed assuming correlated carrier fluctuations throughout the sample.

An estimate of J can be made from published current noise measurements taking $(\Delta V)^2/V^2 = 10^{-15}$ at a frequency of 10 cps for a 20 ohm-cm germanium crystal with ℓ = 5 cm, d = 2.82 x 10^{-2} cm, k = 10^{-16} cm^2, n = 2.5 x 10^{15} cm^{-3} and A = 0.3 cm^2. For a signal-to-noise ratio of 10, J must be of the order of 10^{20} photons/sec or 10 watts. This is much higher than the previous estimate made by assuming the fluctuations were correlated throughout the sample.

APPENDIX V

CURRENT NOISE IN CADMIUM TELLURIDE

by

James J. Brophy and William D. Brennan

IIT RESEARCH INSTITUTE

APPENDIX V

CURRENT NOISE IN CADMIUM TELLURIDE

I. INTRODUCTION

It is well established that resistance fluctuations of a semiconductor caused by random carrier transitions can be investigated by measuring the random noise voltages across the semiconductor when it carries a constant current. Detailed analysis of this current noise data can provide information concerning carrier transition probabilities[1] and the location of discrete trap levels in the forbidden energy gap.[2] Such investigations have been most successful in studying germanium and silicon as well as highly sensitive photoconductors such as cadmium sulfide. A preliminary study of single crystal cadmium telluride specimens has been undertaken here in order to develop information on carrier transitions and trap levels in this material. Such measurements have not previously been reported and, in fact, detailed carrier transitions in cadmium telluride are relatively unknown.

II. CONTACT NOISE

The first specimen investigated, a single crystal p-type specimen, doped (presumably) due to a cadmium deficiency, had a

---

[1] B. V. Rollin and J. P. Russell, Proc. Phys. Soc. 81, 578 (1963); F. M. Klaassen, J. Blok and H. C. Booy, Physica 27, 48 (1961); L. Johnson and H. Levinstein, Phys. Rev. 117, 1191 (1960).

[2] J. J. Brophy, Proceedings of the International Conference on Semiconductor Physics, Prague, 1960; Phys. Rev. 122, 36 (1961).

room temperature resistivity of 70 ohm-cm. The specimen was sandblasted to a conventional four-terminal configuration used in noise studies; the dimensions of the current-carrying portion are 1.6 mm x 2.9 mm x 4 mm. Current contacts and potential probe contacts are provided by etching in a polishing bath consisting of 100 ml HNO_3, 200 ml H_2O, and 40 grams of $K_2CR_2O_7$, and subsequently golding by dipping the ends of the crystal into a solution of gold chloride ($HAUCl_4$). The surface of the semiconductor away from the electrodes is sandblasted.

Current noise voltages appearing at the potential probe contacts were measured and detected using a conventional amplifier-tunable filter-rms vacuum tube voltmeter noise measuring system. Provision was made to vary the magnitude of a resistor in series with the sample's current electrodes in order to investigate the influence of contact noise. Most experiments were carried out with the specimen in the dark, but a small tungsten light bulb was also included in the sample holder to illuminate the specimen for certain measurements.

Preliminary noise spectra observed for this sample show a typical 1/f characteristic, as illustrated in Figure 1 for a current of 100 microamperes. Such a 1/f noise spectrum is characteristic of semiconductors and is also observed at semiconductor-electrode contacts. This type spectra is not generally seen in high resistivity semiconductors such as in cadmium sulfide if the quality of the current contacts is satisfactory. The magnitude of the current noise level

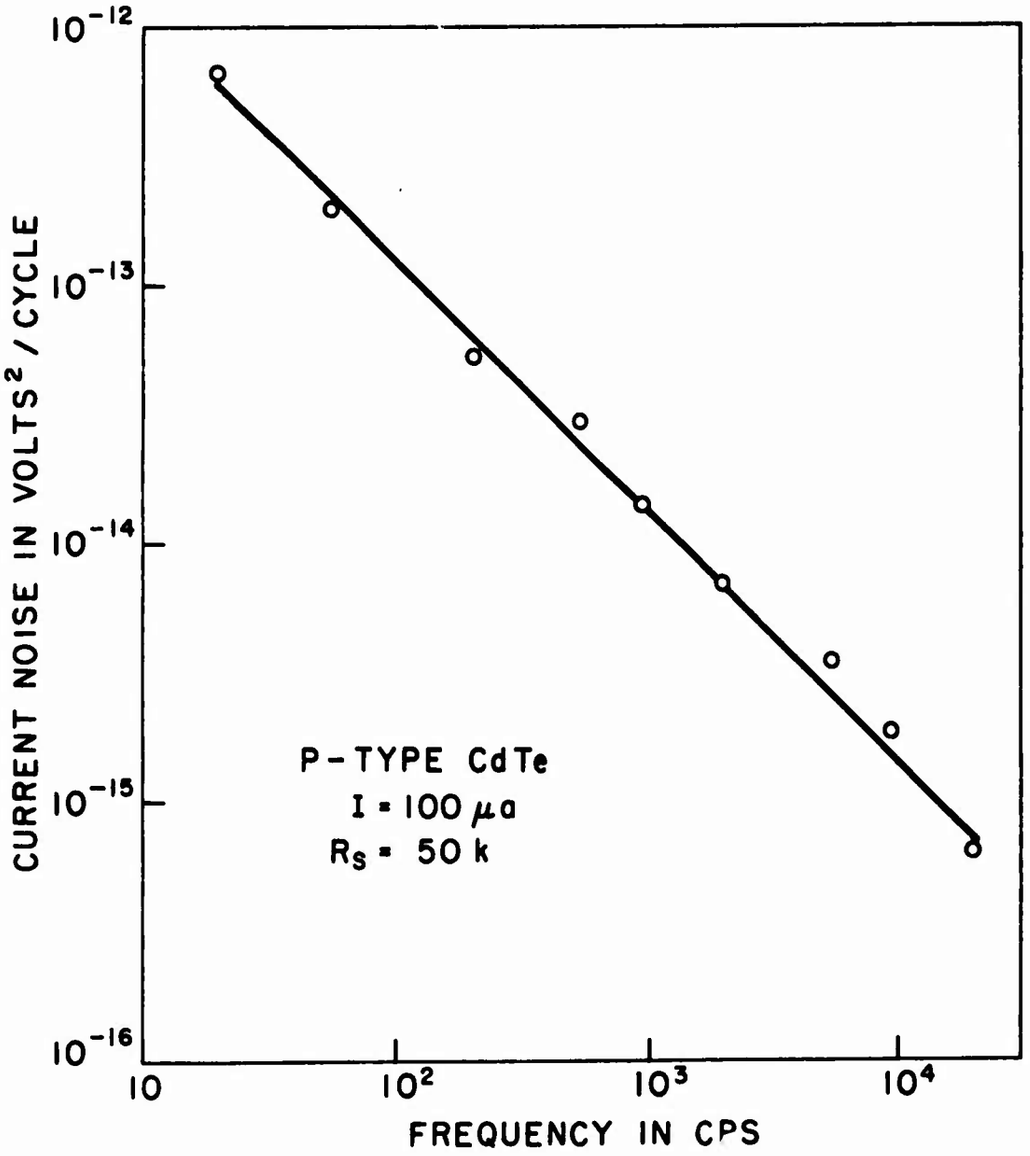

Figure 1. Current Noise Spectrum of P-Type CdTe.

shown in Figure 1 is considerably greater than that generally observed in good quality silicon and germanium single crystals.

The influence of contact noise is investigated by varying the magnitude of a noiseless resistor in series with the sample. In effect, noise voltages observed at the potential probes originate from resistance fluctuations in the semiconductor between the potential probes or current fluctuations caused by extraneous effects such as fluctuations in current contact resistance. Such current fluctuations can be reduced by increasing the value of the series resistance.

A straightforward analysis shows that the noise at the potential probes is given by

$$\langle \Delta V^2 \rangle = \frac{I^2 \langle \Delta R^2 \rangle}{(1 + R/R_S)^2} + \frac{\langle \Delta V_E^2 \rangle}{(1 + R_S/R)^2} \qquad (1)$$

where $\langle \Delta V^2 \rangle$ is the random noise voltage measured between the sample potential probes, I is the sample current, R and $\langle \Delta R^2 \rangle$ are the average and fluctuations in the sample resistance, R_S is the series resistance, and $\langle \Delta V_E^2 \rangle$ is the extraneous noise.

In Equation (1) the first term represents the desired measurement of resistance fluctuations while the second term accounts for extraneous noise effects. As the value of R_S is increased, the observed noise level reaches a plateau characteristic of the semiconductor independent of the extraneous noise sources. The approach to the desired plateau may be concave upward or concave downward, depending upon the relative magnitudes of the extraneous noise and

$I^2 \langle \Delta R^2 \rangle$. The situation in which the observed noise rises to a plateau is desirable, indicative of good quality contacts, and is generally observed in silicon and germanium specimens.[3] Even in the case of noisy current contacts, however, a satisfactory contact-current plateau can sometimes be obtained,[4] which can be used to investigate current noise characteristic of the semiconductor.

Variation of the current noise at the potential probes as a function of series resistance for the cadmium telluride specimen is illustrated in Figure 2 at a frequency of 1 kc and for a sample current of 100 μa. The upper curve in Figure 2 illustrates the noise levels observed for the first set of contacts produced on this specimen. A very large noise level at small values of R_S indicates that the current contacts are extremely noisy. A plateau at large values of R_S is indicated, but this plateau is not greater than the Nyquist noise level of the specimen. This means that it is not possible to measure current noise characteristic of resistance fluctuations in excess of Nyquist noise at this frequency and current. The solid line in Figure 2 represents Equation (1) computed for a sample resistance of 2×10^4 ohms, as measured separately. Good agreement between predicted and observed results is apparent.

---

[3] J. J. Brophy, Solid-State Physics in Electronics and Telecommunications (Academic Press, Inc., New York, 1960), p. 548.

[4] J. J. Brophy, J. Appl. Phys. 33, 114 (1962).

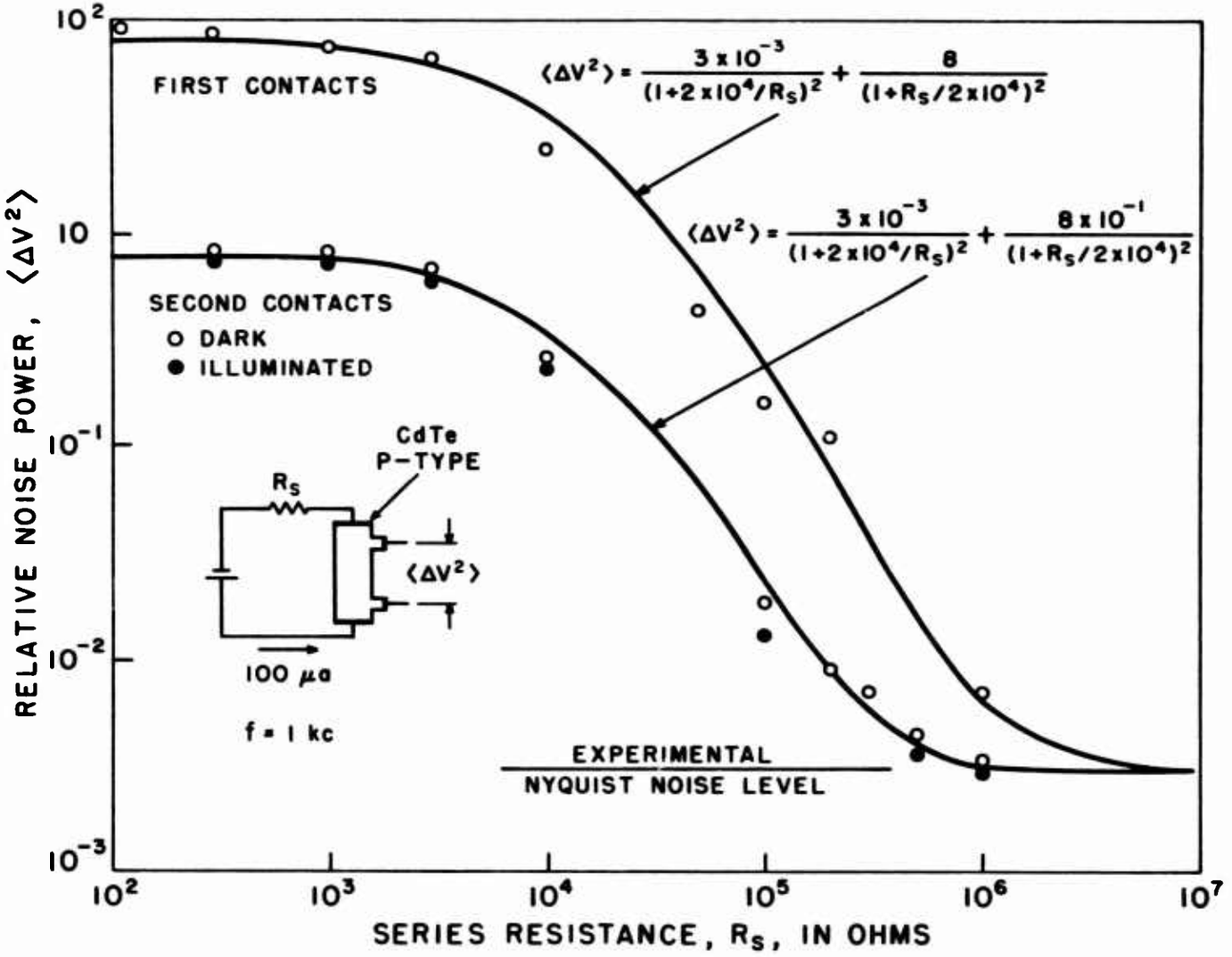

Figure 2. Variation of Measured Current Noise Level with Series Resistance Showing Influence of Noisy Contacts. Curves are Analytical and Data Points Experimental.

During the later stages of this work, one of the sample contacts was inadvertently disturbed. Upon reworking this contact, the lower curve in Figure 2 was observed. Here again, the solid line reporesents Equation (1) while the data points are experimental. These results show that contact noise has been reduced by one order of magnitude. It is still not possible to observe current noise characteristic of the semiconductor in excess of Nyquist noise, however. In the hope of increasing the resistance fluctuations in the body of the semiconductor, the sample was illuminated with white light from a tungsten bulb. The solid data points in Figure 2 represent this data. Little change between the dark and illuminated condition is observed. This is consistent with the relatively small photoconductive effect observed in this specimen. Clearly, the carrier transitions induced by illumination are not sufficient to increase resistance fluctuations to an observable level.

On the basis of this preliminary investigation of current noise in this single crystal cadmium telluride specimen, it is clear that the contacts are extremely noisy. The current noise results show this very definitely even though the contacts are fairly satisfactory by other normal measuring techniques. The data in Figure 2 illustrate that relatively minor changes in electrodes produce major changes in the contact noise. This suggests that further study of contacting techniques is appropriate. Furthermore, the current noise measurements are extremely sensitive tests for electrode quality.

Because of the influence of contact noise, it is not possible to observe bulk noise effects. That is, the current noise level at currents of 100 μa is not in excess of Nyquist noise. It is not possible to increase the magnitude of the dc current since this also increases the contact noise level. However, after sufficiently lower noise contacts are produced, increased dc current should improve the situation considerably. In addition, the surface of the semiconductor can be etched to determine if an increase in current noise is observed, as is the case for germanium and silicon.

III. RESISTANCE FLUCTUATIONS

A second sample investigated has a resistivity of 2.9×10^4 ohm-cm. This sample is n-type, presumably due to tellurium deficiency. The specimen was provided with similar contacts and cut into the same shape used previously.

As shown in Figure 3, contact noise is relatively less significant in this specimen than for the p-type sample. An appreciable amount of contact noise is still present, but it is possible to achieve sufficiently constant current conditions at high values of series resistance to investigate resistance fluctuations characteristic of the semiconductor.

The current noise spectra of this crystal are shown in Figure 4 for the sample in the dark and strongly illuminated at a wavelength just beyond the fundamental absorption edge. In the absence of current flow white Nyquist noise is observed as expected and the noise level is lower upon illumination, indicative of a small

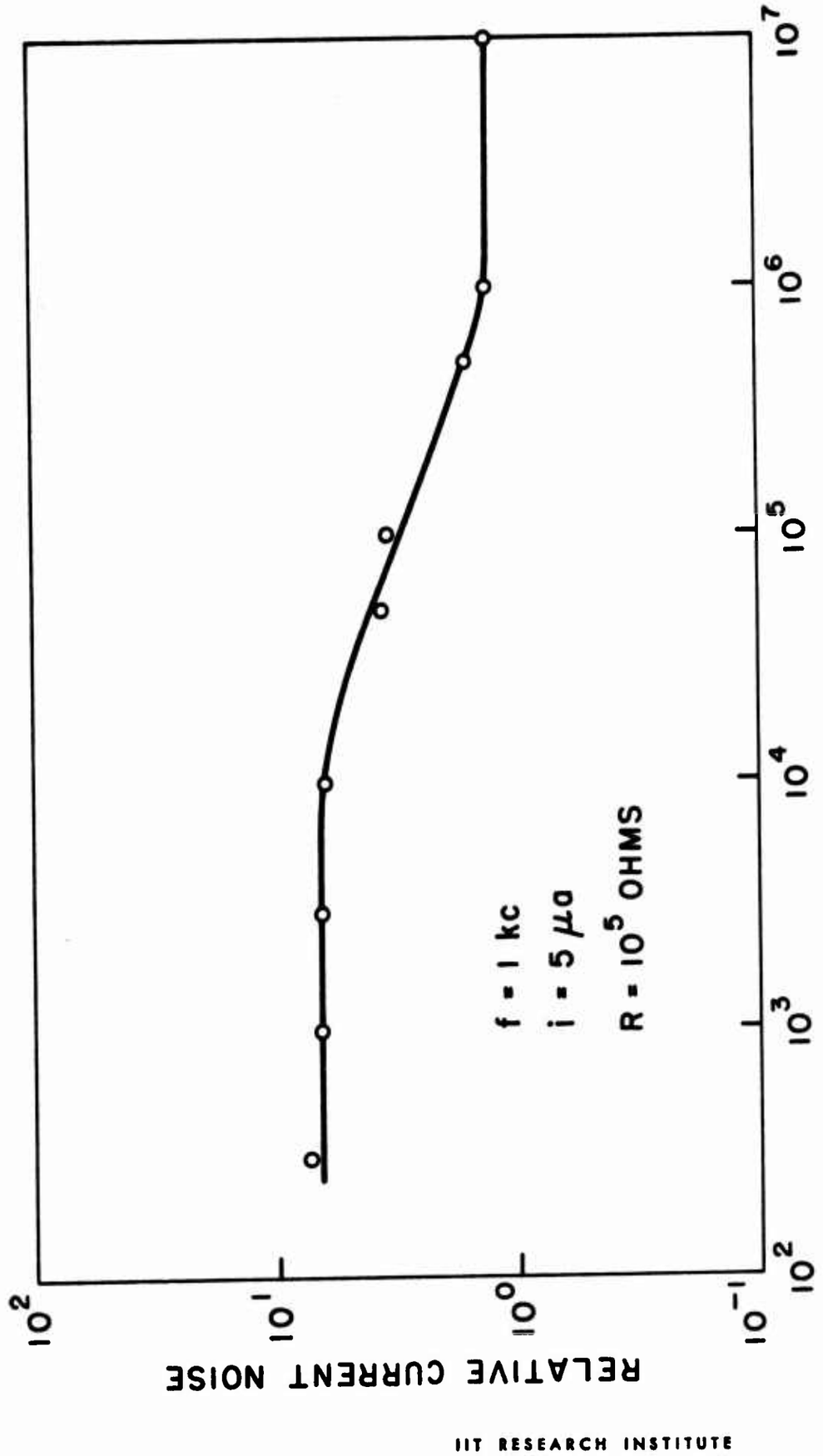

Figure 3. Variation of Current Noise with Series Resistance for High Resistivity n-Type CdTe.

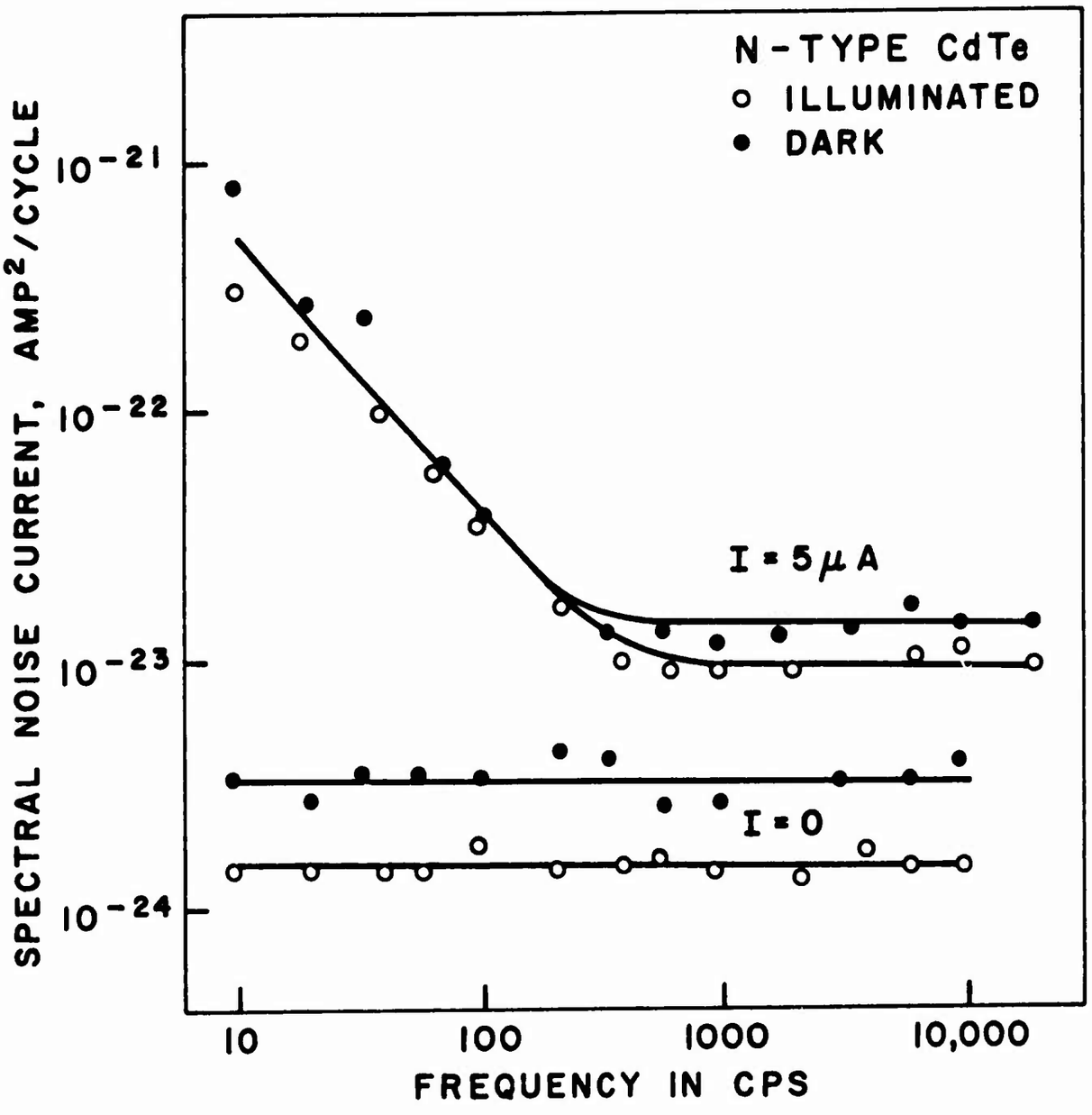

Figure 4. Noise Spectra of n-Type CdTe Single Crystal in the Dark and Under Illumination.

but significant photoconductivity. In the presence of current a low frequency 1/f noise component is apparent together with increased white noise at high frequencies. It is significant that the low frequency noise is unaffected by illumination which suggests that this component is a result of residual contact noise. The white noise component is reduced by illumination which is rather the reverse effect from that seen in other photoconductors.

The variation of noise level with current in both the dark and illuminated condition is shown in Figure 5. The variation is essentially linear at low currents and square-law at higher currents. Based on the known presence of contact noise, the high current portion is attributed to 1/f noise associated with the contacts. In addition, this data again shows that the noise under illumination is lower than that with the sample in the dark.

Ignoring the 1/f noise component associated with the contacts, Figures 4 and 5 show a white noise component which increases linearly with the current and is reduced upon illumination. Both the current dependence and the effect of illumination suggests that the usual interpretation of current noise in photoconductors[1] based on generation-recombination transitions is inappropriate. Rather, the limited data available suggests that the observed noise is simple shot noise.

The expected shot noise level corresponding to 5 microamperes is 1.6×10^{-24} amp^2/cycle. This is somewhat smaller than the observed noise level in Figure 4 of about 8×10^{-24} amp^2/cycle. Part of

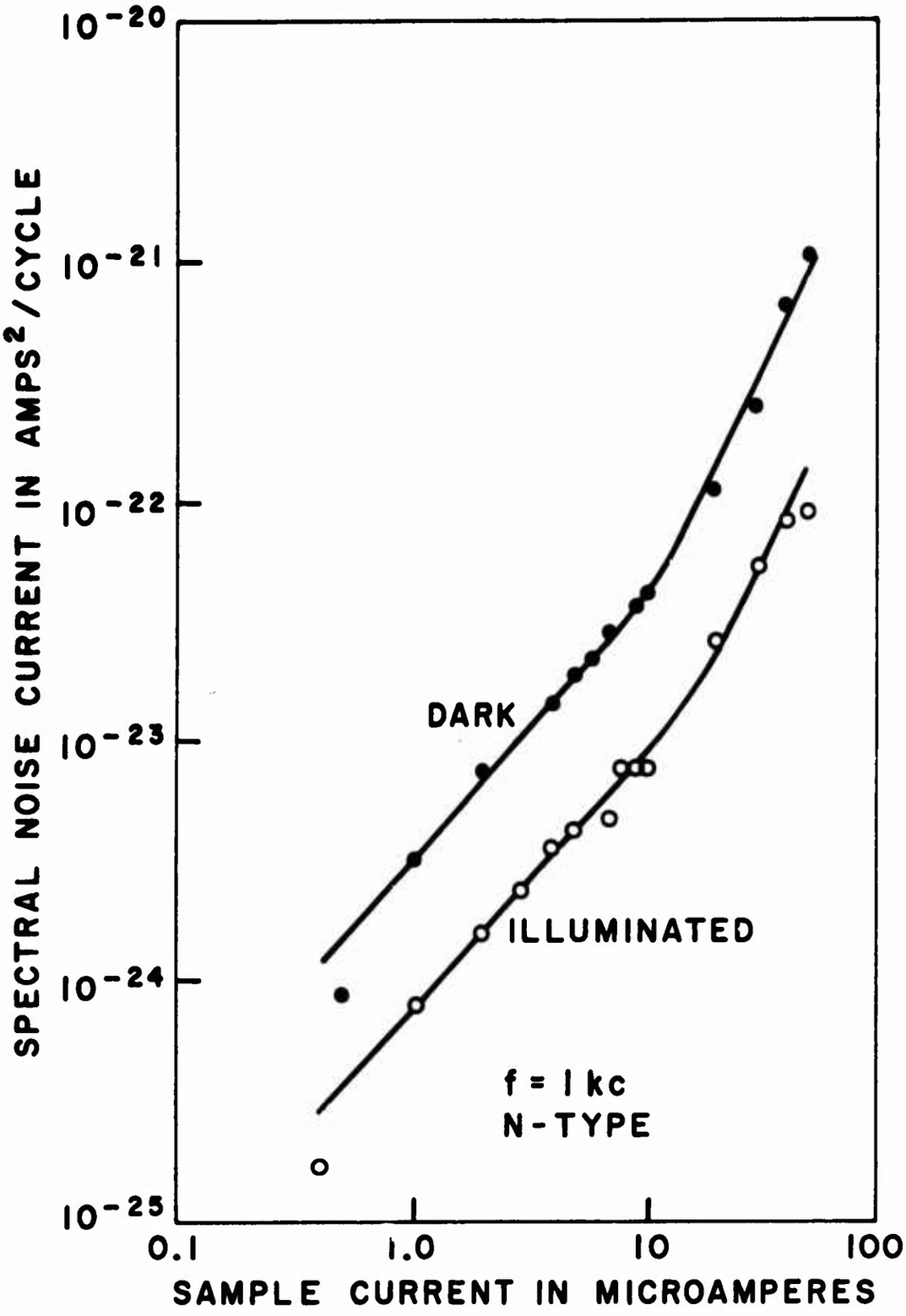

Figure 5. Current Noise in an n-Type Cadmium Telluride Single Crystal.

the discrepancy may be a result of inaccurate determination of the effective sample resistance between potential probe side arms. However, the discrepancy seems larger than can be accounted for on this basis. It is tempting to suggest that the observed noise is, in fact, shot noise but increased somewhat over the simple shot noise expression as a result of sample inhomogeneity. This explanation m also account for the lower noise level upon illumination, since the inhomogeneities would tend to be reduced by the additional carriers produced photoelectrically.

The results of this preliminary investigation of current noise in cadmium telluride show that electrode problems are quite severe. With suitable care, however, it is possible to obtain noise data characteristic of the bulk conduction processes. The present data suggests that the main features of noise observed in high resistivity specimens can be explained by simple shot noise. If this is so, it will be the first time that shot noise has been observed in a bulk semiconductor.

Unclassified
Security Classification

DOCUMENT CONTROL DATA - R&D
(Security classification of title, body of abstract and indexing annotation must be entered when the overall report is classified)

1. ORIGINATING ACTIVITY (Corporate author)	2a. REPORT SECURITY CLASSIFICATION
IIT Research Institute 10 West 35th Street Chicago, Illinois 60616	Unclassified
	2b. GROUP

3. REPORT TITLE

"EXCESS NOISE IN SEMICONDUCTORS"

4. DESCRIPTIVE NOTES (Type of report and inclusive dates)

Annual Summary Report covering 15 November 1965 to 14 November 1966

5. AUTHOR(S) (Last name, first name, initial)

Brophy, James J.

6. REPORT DATE	7a. TOTAL NO. OF PAGES	7b. NO. OF REFS
14 November 1966	81	28

8a. CONTRACT OR GRANT NO.	9a. ORIGINATOR'S REPORT NUMBER(S)
NOOO14-66-C0032 b. PROJECT NO.	Project A6145 Annual Summary Report No. 1
c. d.	9b. OTHER REPORT NO(S) (Any other numbers that may be assigned this report) None

10. AVAILABILITY/LIMITATION NOTICES

Qualified requesters may obtain copies of this report from DDC.

11. SUPPLEMENTARY NOTES	12. SPONSORING MILITARY ACTIVITY
None	Office of Naval Research, Physics Branch, Department of the Navy, Washington 25, D. C.

13. ABSTRACT

Optical emission fluctuations in luminescent p-n junctions are correlated with the forward current noise of the junction. When appreciable carrier recombination in the space charge region exists, characteristic time constants associated with recombination transitions are observed in the noise spectra. In other diodes, both the forward current noise and the optical emission noise exhibit a 1/f spectra. It is found that diodes in which the forward current is carried by diffusion do not show optical emission noise beyond statistical photon fluctuations.

It is possible to determine essentially all of the important junction parameters of luminescent p-n junctions through combined electrical and optical measurements. This is so because of the good agreement between simple p-n junction theory and experimental results. The parameters which can be obtained are junction area, width, internal potential, saturation current, and impurity content.

A preliminary study of current noise in single crystal CdTe shows that contact noise is significant and that bulk noise may be interpreted in terms of shot noise associated with crystalline inhomogeneity.

DD FORM 1 JAN 64 1473

Unclassified
Security Classification

Unclassified

Security Classification

14. KEY WORDS	LINK A		LINK B		LINK C	
	ROLE	WT	ROLE	WT	ROLE	WT
OPTICAL FLUCTUATIONS						
ELECTROLUMINESCENT JUNCTIONS						
P-N JUNCTIONS						
CURRENT NOISE						
CADMIUM TELLURIDE						

INSTRUCTIONS

1. **ORIGINATING ACTIVITY:** Enter the name and address of the contractor, subcontractor, grantee, Department of Defense activity or other organization *(corporate author)* issuing the report.

2a. **REPORT SECURITY CLASSIFICATION:** Enter the overall security classification of the report. Indicate whether "Restricted Data" is included. Marking is to be in accordance with appropriate security regulations.

2b. **GROUP:** Automatic downgrading is specified in DoD Directive 5200.10 and Armed Forces Industrial Manual. Enter the group number. Also, when applicable, show that optional markings have been used for Group 3 and Group 4 as authorized.

3. **REPORT TITLE:** Enter the complete report title in all capital letters. Titles in all cases should be unclassified. If a meaningful title cannot be selected without classification, show title classification in all capitals in parenthesis immediately following the title.

4. **DESCRIPTIVE NOTES:** If appropriate, enter the type of report, e.g., interim, progress, summary, annual, or final. Give the inclusive dates when a specific reporting period is covered.

5. **AUTHOR(S):** Enter the name(s) of author(s) as shown on or in the report. Enter last name, first name, middle initial. If military, show rank and branch of service. The name of the principal author is an absolute minimum requirement.

6. **REPORT DATE:** Enter the date of the report as day, month, year; or month, year. If more than one date appears on the report, use date of publication.

7a. **TOTAL NUMBER OF PAGES:** The total page count should follow normal pagination procedures, i.e., enter the number of pages containing information.

7b. **NUMBER OF REFERENCES:** Enter the total number of references cited in the report.

8a. **CONTRACT OR GRANT NUMBER:** If appropriate, enter the applicable number of the contract or grant under which the report was written.

8b, 8c, & 8d. **PROJECT NUMBER:** Enter the appropriate military department identification, such as project number, subproject number, system numbers, task number, etc.

9a. **ORIGINATOR'S REPORT NUMBER(S):** Enter the official report number by which the document will be identified and controlled by the originating activity. This number must be unique to this report.

9b. **OTHER REPORT NUMBER(S):** If the report has been assigned any other report numbers *(either by the originator or by the sponsor)*, also enter this number(s).

10. **AVAILABILITY/LIMITATION NOTICES:** Enter any limitations on further dissemination of the report, other than those imposed by security classification, using standard statements such as:

(1) "Qualified requesters may obtain copies of this report from DDC."

(2) "Foreign announcement and dissemination of this report by DDC is not authorized."

(3) "U. S. Government agencies may obtain copies of this report directly from DDC. Other qualified DDC users shall request through _____."

(4) "U. S. military agencies may obtain copies of this report directly from DDC. Other qualified users shall request through _____."

(5) "All distribution of this report is controlled. Qualified DDC users shall request through _____."

If the report has been furnished to the Office of Technical Services, Department of Commerce, for sale to the public, indicate this fact and enter the price, if known.

11. **SUPPLEMENTARY NOTES:** Use for additional explanatory notes.

12. **SPONSORING MILITARY ACTIVITY:** Enter the name of the departmental project office or laboratory sponsoring *(paying for)* the research and development. Include address.

13. **ABSTRACT:** Enter an abstract giving a brief and factual summary of the document indicative of the report, even though it may also appear elsewhere in the body of the technical report. If additional space is required, a continuation sheet shall be attached.

It is highly desirable that the abstract of classified reports be unclassified. Each paragraph of the abstract shall end with an indication of the military security classification of the information in the paragraph, represented as *(TS), (S), (C), or (U)*.

There is no limitation on the length of the abstract. However, the suggested length is from 150 to 225 words.

14. **KEY WORDS:** Key words are technically meaningful terms or short phrases that characterize a report and may be used as index entries for cataloging the report. Key words must be selected so that no security classification is required. Identifiers, such as equipment model designation, trade name, military project code name, geographic location, may be used as key words but will be followed by an indication of technical context. The assignment of links, roles, and weights is optional.

DD FORM 1 JAN 64 1473 (BACK)

Unclassified

Security Classification